

**FACULDADE DE ENGENHARIA DA UNIVERSIDADE DO PORTO**



# **Development of a Circuit Breaker Health Index Algorithm and Real-time closed-loop Testing**

**André Filipe de Sousa Martins**

Mestrado Integrado em Engenharia Eletrotécnica e de Computadores

Supervisor: Helder Filipe Duarte Leite, PhD

July 23, 2021



# Resumo

O disjuntor é uma parte essencial em subestações de alta tensão, contribuindo para a proteção de toda a rede elétrica. A sua condição tem de ser garantida de forma a prevenir falhas inesperadas e consequente paragem de partes da subestação. Por essa razão, devem ser constantemente monitorizados e, quando necessário, reparados ou substituídos.

Hoje em dia, a monitorização é principalmente feita por dispositivos eletrónicos inteligentes, também denominados de relés digitais, que guardam a informação recolhida de sensores e transformadores de corrente/tensão, podendo ser posteriormente acedida pela gestão da subestação. Isso foi possível devido à introdução das normas IEC 61850 e COMTRADE, que permitiram a integração dos sistemas de automação em subestações e facilitaram a troca de informação entre o diverso equipamento presente dentro de uma subestação.

Tirando partido desses protocolos, denominadamente do protocolo COMTRADE, um teste em malha fechada em tempo real é efetuado de modo a simular o comportamento de um disjuntor durante a sua operação de abertura. Para esse efeito, um programa de simulação de transientes eletromagnéticos em tempo real é utilizado, juntamente com um amplificador de sinal ligado a um relé digital, que exporta os sinais simulados para processamento e análise. Com essa informação, um algoritmo de índice de saúde é criado para avaliar a condição do disjuntor em estudo. Este índice possui parâmetros *online*, possíveis de recolher durante o funcionamento normal do disjuntor, e parâmetros *offline* mais específicos, baseados em testes de estado de arte feitos a disjuntores de alta tensão, resultando desse modo o estado geral do disjuntor simulado em questão.

**Palavras-chave:** Disjuntor; Teste em malha fechada; Índice de saúde; Arco elétrico.





# Abstract

Circuit breakers are a key part of high-voltage substations, contributing to the protection of the entire electrical grid. Their good condition must be guaranteed to prevent unexpected failures and consequent shutdown of parts of the substation. For that reason, they need to be constantly monitored and, when necessary, repaired or replaced.

The monitoring nowadays is mainly done by intelligent electronic devices, which record data coming from sensors and current/voltage transformers for the substation management to have access to that information. That was possible with the introduction of the IEC 61850 and COMTRADE standards, which allowed the integration of substation automation systems and facilitated the exchange of information between the different equipment inside a substation.

By taking advantage of these protocols, particularly the COMTRADE standard, a real-time closed-loop test is done to simulate the behaviour of a circuit breaker during its opening operation. For that effect, a real time electromagnetic transient program is used, together with a signal amplifier connected to a digital relay, which outputs the simulated data for processing and analysis. With that information, a health index algorithm is created to evaluate the condition of the breaker being studied. This index consists of online parameters, able to be collected during the normal functioning of the circuit breaker, and more specific offline parameters, based on state-of-the-art tests done to high-voltage breakers, providing a overall current state of the simulated circuit breaker.

**Keywords:** Circuit breaker; Closed-loop test; Health Index; Switching arc.



# Acknowledgements

I would like to thank Prof. Helder for all the guidance given to me during the whole dissertation. I would also like to thank Eng. Cláudio Silva, Eng. Rui Jorge and Eng. Rui Nogueira from Efacec for the help given with the IED and the fast response to the problems that appeared initially.

Most importantly though, I would like to thank my parents, my brother and Daniela, which were always there for me when I needed during all these years, and supported me during every step and decision I took. For that, I owe them the world.

Thank you all,

André Martins



*“Be who you are and say what you feel,  
because those who mind don’t matter,  
and those who matter don’t mind.”*

Bernard M. Baruch



# Contents

<b>1</b>	<b>Introduction</b>	<b>1</b>
1.1	Motivation and Purpose . . . . .	1
1.2	Structure and Organization . . . . .	2
<b>2</b>	<b>Electric Arc Modelling in Circuit Breakers</b>	<b>3</b>
2.1	Circuit Breaker . . . . .	3
2.2	Functioning and Design of a Circuit Breaker . . . . .	3
2.3	Types of Circuit Breakers . . . . .	4
2.4	Switching Arc in a Circuit Breaker . . . . .	5
2.4.1	Tripping the Circuit Breaker in Alternating Current . . . . .	6
2.4.2	Transient Recovery Voltage in the opening of the Circuit Breaker . . . . .	7
2.4.3	Mathematical Models used for modelling the Electric Arc . . . . .	8
2.5	Summary . . . . .	16
<b>3</b>	<b>IEC 61850 based disturbance and fault recorder for Electric Arc Modelling in Circuit Breakers</b>	<b>17</b>
3.1	Substation Automation Systems and IEC 61850 . . . . .	17
3.1.1	IEC 61850 System Configuration Description Language . . . . .	18
3.1.2	IEC 61850 Basic Information and Communication Structure . . . . .	20
3.2	Common format for Transient Data Exchange for power systems (COMTRADE)	24
3.2.1	COMTRADE File Types . . . . .	24
3.3	Summary . . . . .	29
<b>4</b>	<b>Real-time closed-loop Testing for Electric Arc Modeling in Circuit Breakers</b>	<b>31</b>
4.1	Real Time Digital Simulator . . . . .	31
4.1.1	RTDS Software Description . . . . .	32
4.1.2	RTDS Hardware Description . . . . .	33
4.1.3	Circuit Breaker Electric Arc Model Simulation . . . . .	36
4.2	Doble F6350e Signal Amplifier . . . . .	39
4.3	Finalizing the closed-loop test by recording the simulated disturbances . . . . .	40
4.4	Summary . . . . .	42
<b>5</b>	<b>Creating the Health Index for the Circuit Breaker</b>	<b>43</b>
5.1	Online Parameters Analysis . . . . .	44
5.1.1	Circuit Breaker Opening Time . . . . .	44
5.1.2	Current Root Mean Square Value after Circuit Breaker opening . . . . .	48
5.1.3	Transient Recovery Voltage duration . . . . .	51
5.1.4	Weighting the Online Parameters . . . . .	53

5.2	Offline Parameters Analysis . . . . .	55
5.2.1	Dynamic contact Resistance Measurement . . . . .	55
5.2.2	Time-travel analysis . . . . .	57
5.2.3	Minimum pick-up Voltage . . . . .	59
5.3	Summary . . . . .	59
<b>6</b>	<b>Main Conclusions and Limitations</b>	<b>61</b>
<b>A</b>	<b>RSCAD Draft Scheme</b>	<b>63</b>
<b>B</b>	<b>RSCAD Runtime Scheme</b>	<b>65</b>
	<b>References</b>	<b>67</b>



# List of Figures

2.1	SF <sub>6</sub> single-pressure modular until capable of interrupting 31 kA at 107 kV . . . .	4
2.2	V/I characteristic of the electric arc in DC . . . . .	5
2.3	Typical variations of current and voltage showing the peak of extinction voltage $e_s$ and peak of re-ignition voltage $e_r$ . . . . .	6
2.4	Grid voltage, short-circuit current, arc voltage and voltage measured between the circuit breaker terminals . . . . .	6
2.5	Transient Recovery Voltage of a resistive, inductive and capacitive circuit . . . .	7
2.6	Transient Recovery Voltage: a) Current Zero; b) Maximum Current . . . . .	8
2.7	Schematic used to simulate the Circuit Breaker electric arc in PSCAD <sup>TM</sup> /EMTDC <sup>TM</sup>	10
2.8	External object used to simulate the Mayr, Cassie and Schavemaker arc models' behaviour . . . . .	11
2.9	Values used for the constants in the Mayr Arc Model implementation . . . . .	11
2.10	Current and Voltage obtained in the Mayr Arc Model Simulation . . . . .	12
2.11	Mayr simulation's Voltage and Current in the moment of Circuit Breaker opening	12
2.12	Values used for the constants in the Cassie Arc Model implementation . . . . .	13
2.13	Cassie simulation's Voltage and Current in the moment of Circuit Breaker opening	13
2.14	Current and Voltage obtained in the Cassie Arc Model Simulation . . . . .	14
2.15	Values used for the constants in the Schavemaker Arc Model implementation . .	15
2.16	Schavemaker simulation's Voltage and Current in the moment of Circuit Breaker opening . . . . .	15
2.17	Current and Voltage obtained in the Schavemaker Arc Model Simulation . . . . .	16
3.1	Configuration of substation automation system and data exchange . . . . .	18
3.2	Structure of a SCL configuration file . . . . .	19
3.3	Substation engineering process with SCL files . . . . .	20
3.4	ACSI server building block . . . . .	21
3.5	ACSI communication model . . . . .	22
3.6	SPS class . . . . .	23
3.7	Circuit Breaker Logical Node Definition . . . . .	23
3.8	Data Object Definition for a Circuit Breaker operating capability . . . . .	24
3.9	Record set with all four different file types . . . . .	24
3.10	Header file example . . . . .	25
3.11	Configuration file example . . . . .	26
3.12	Data file example in ASCII . . . . .	28
3.13	Data sample in binary format example . . . . .	28
3.14	Information file example . . . . .	29
4.1	Equipment setup for closed-loop testing . . . . .	31

4.2	RSCAD Fileman Overview . . . . .	32
4.3	Circuit Breaker Arc Model component built in CBuilder . . . . .	33
4.4	Front panel of the Processor Cards available in the RTDS rack used . . . . .	34
4.5	WIF Front Panel . . . . .	35
4.6	GTAI and GTAO 16-bit analog ports . . . . .	36
4.7	Scheme made in RSCAD/Draft to implement the Circuit Breaker electric arc model . . . . .	36
4.8	Voltage and Current measurements in all three phases in RSCAD/Runtime . . . . .	37
4.9	Single Phase Voltage and Current measurements in the Circuit Breaker . . . . .	38
4.10	Doble F6350e Signal Amplifier . . . . .	39
4.11	Configuration of the F6350e Amplifier . . . . .	39
4.12	Cable used to inject Low-Level Signals into the Signal Amplifier . . . . .	40
4.13	TPU D500 . . . . .	40
4.14	Connection between the F6530e and the TPU D500 . . . . .	41
4.15	3-Phase Current measured during the recorded disturbance . . . . .	41
4.16	3-Phase Voltage measured during the recorded disturbance . . . . .	42
4.17	Interaction between all the equipment in the closed-loop test . . . . .	42
5.1	Waveforms of all three phases' current during a recorded disturbance . . . . .	43
5.2	Waveforms of all three phases' voltage during a recorded disturbance . . . . .	44
5.3	Opening Time measurement procedure . . . . .	45
5.4	Opening Time normal distribution applied to the sampled data . . . . .	45
5.5	Distribution of all records' Opening Time performance . . . . .	46
5.6	Voltage and Current plots of an opening with good performance results . . . . .	46
5.7	Voltage and Current plots of an opening with poor performance results . . . . .	47
5.8	Current RMS value measurement procedure . . . . .	48
5.9	Current RMS Value normal distribution applied to the sampled data . . . . .	49
5.10	Distribution of all records' Current RMS Value performance . . . . .	49
5.11	Voltage and Current plots of two distinct RMS measurement recordings . . . . .	50
5.12	Comparison between the voltage waveform of a signal and its wavelet transform . . . . .	51
5.13	TRV duration measurement procedure . . . . .	52
5.14	TRV duration Value normal distribution applied to the sampled data . . . . .	53
5.15	Distribution of all records' TRV duration performance . . . . .	53
5.16	Total performance of all recordings . . . . .	54
5.17	Comparison between rated and low speed in the dynamic resistance measurement . . . . .	55
5.18	Typical DRM curve with the diagnosis features . . . . .	56
5.19	Circuit Breaker operating tests . . . . .	58
5.20	Typical closing operation parameters analysed . . . . .	58
5.21	Voltage and Current waveforms of a typical minimum pick-up voltage measurement . . . . .	59
5.22	Decision tree of the Full Health Indexing of a Circuit Breaker . . . . .	60

# Abbreviations

<b>AC</b>	Alternating Current
<b>ACSI</b>	Abstract communication service interface
<b>CB</b>	Circuit Breaker
<b>CDC</b>	Common Data Classes
<b>COMTRADE</b>	Common format for Transient Data Exchange for power systems
<b>DAC</b>	Digital-to-Analog Converter
<b>DC</b>	Direct Current
<b>DRM</b>	Dynamic contact Resistance Measurement
<b>EMTP</b>	Electromagnetic Transients Program
<b>GPC</b>	Giga-Processor Card
<b>GTAI</b>	Gigabit Transceiver Analogue Input Card
<b>GTAO</b>	Gigabit Transceiver Analogue Output Card
<b>I&amp;C</b>	Instrumentation and Control
<b>ICD</b>	IED Capability Description
<b>IEC</b>	International Electrotechnical Commission
<b>IED</b>	Intelligent Electronic Device
<b>IID</b>	Instantiated IED Description
<b>LN</b>	Logical Node
<b>RRRV</b>	Rate of Rise of Recovery Voltage
<b>RTDS</b>	Real Time Digital Simulator
<b>SAS</b>	Substation Automated Systems
<b>SCD</b>	Substation Configuration Description
<b>SCL</b>	System Configuration description Language
<b>SED</b>	System-exchange Description
<b>SSD</b>	System/Substation Specification Description
<b>SPS</b>	Single Point Status
<b>TRV</b>	Transient Recovery Voltage
<b>WIF</b>	Workstation Interface Card
<b>3PC</b>	Triple Processor Card



# Chapter 1

## Introduction

### 1.1 Motivation and Purpose

Power system disturbances have a relevant impact on electrical substations, as the possible service downtime results in big financial losses to the substation management. Because of that, utilities are now recognizing that the power system and Instrumentation Control (I&C) system assets, such as cables, transformers, breakers, and control systems, require more visibility.

More specifically, the circuit breaker (CB) is an important asset regarding the protection of the whole substation and its equipment. For that effect, however, it needs to be properly monitored, maintained, and eventually replaced.

Nowadays, monitoring information in substations goes to digital relays also known as Intelligent Electronic Devices (IED). Data for analysis include operating conditions of the power system such as metering and status, operating parameters of power system devices such as circuit breaker and transformer conditions, IED self-test diagnostics. Analysis data also include archived records representing the reaction of the power system over time or to an event; these include system profiles, event reports, sequential events recorder files, power quality reports, and protection quality reports.

Collected information is often not used to predict maintenance schedules or to make operations or construction decisions. Data available from an integrated system of IEDs can serve many purposes including equipment health monitoring.

The goal of this work is to collect monitoring data from the IED regarding a CB, more specifically the COMTRADE files of its recorded disturbances, and use them to determine the condition of the breaker, through the formulation of a health index, and with it take the necessary actions regarding maintenance/replacement.

## 1.2 Structure and Organization

The first Chapter presents the main topics covered on this work, providing its context and objectives. In addition to that, it also details how this report is structured, giving an overview of the subjects covered by each chapter.

Chapter 2 introduces the circuit breaker regarding its functioning and design. In addition to that, it also explains some mathematical models used for modelling the electric arc created during an opening operation, together with their implementation in PSCAD<sup>TM</sup>/EMTDC<sup>TM</sup>.

In Chapter 3, the standards which are the bases for IED integration in substations and obtaining information about its assets are explained, detailing how they can be used to collect data from the CB and analyse it.

Chapter 4 presents the closed-loop scheme used to simulate the behaviour of the breaker in real time, demonstrating the results obtained in each part of the process.

Chapter 5 addresses the creation of the health index algorithm, using the data collected from the closed-loop simulations, and evaluating the overall state of the breaker being analysed.

Finally, Chapter 6 presents the final conclusions on this work and the limitations existent during the entire procedure.

## Chapter 2

# Electric Arc Modelling in Circuit Breakers

In this chapter, the functioning of a circuit breaker is explained, presenting its design and state-of-the-art most predominant types existent in high-voltage substations.

The opening operation of a breaker is also addressed, detailing the behaviour of the electric arc created during this process and its relevant parameters. Moreover, some mathematical models used to reproduce it in simulation environments are mentioned.

### 2.1 Circuit Breaker

A circuit breaker, as the name suggests, is used to close off the power supply section when any abnormal condition occurs, such as current faults. This way, the power supply is isolated from the faulty equipment avoiding further damages to the grid [1].

In high-voltage substations, CBs are connected to protective relays which detect fault conditions in the grid and order the respective CB to trip [2].

### 2.2 Functioning and Design of a Circuit Breaker

The circuit breaker possesses two stable conditions, one of them being "close", in which it has ideally zero, and in practice a very small impedance, letting current go through it, and "open", having ideally an infinite and practically an extremely high impedance. The switching element in such a device, the impedance of which is caused to change, may take the form of a resistance, inductance or capacitive impedance. [3]

In most CBs, this variable impedance is a high pressure arc. It acts as a variable resistor, and the art and science of CB design is to control the arc so that its resistance varies with current in such a way that satisfactory current interruption will be obtained. For alternating current (AC) breakers, there are two current zeros every cycle, and most of the designers aim to maintain a high-conductance arc during the period of current flow, to minimise the energy dissipated in the CB and

to cause the conductance of the arc to decrease extremely rapidly a few microseconds before the current zero. The designer's problem is to control the arc so that the energy-removal processes at the current zero are sufficiently intense to raise the resistance of the arc rapidly enough at the current zero to prevent reignition when interrupting large fault currents, and yet are not so intense that small currents are "chopped" before the current zero, giving rise to high overvoltages. [4]

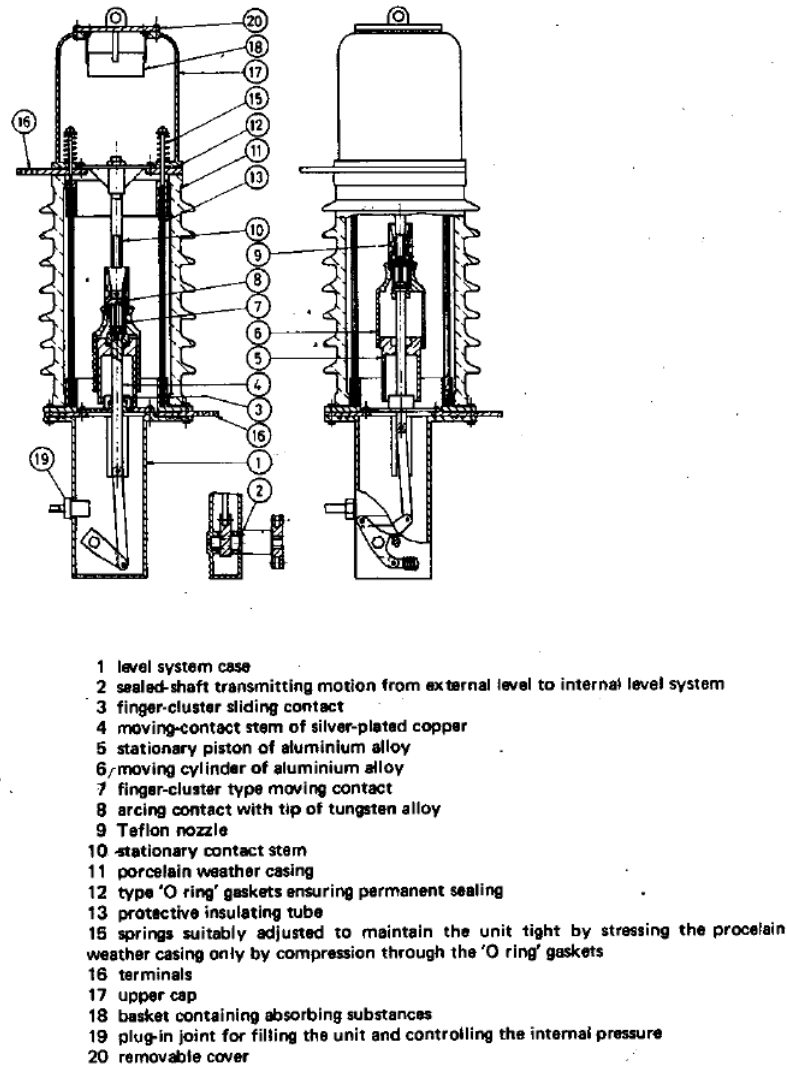


Figure 2.1: SF<sub>6</sub> single-pressure modular unit capable of interrupting 31 kA at 107 kV [5]

## 2.3 Types of Circuit Breakers

The circuit breakers used in the distribution systems are: [6]

**Air CB:** The air is used as the arc extinguish medium, having good insulation properties at normal temperatures and being freely available. However, there are some problems with this



kind of CB, as the power arc being drawn in the air raises a considerable volume of air to high temperatures, making the cooling of the actual ionised path difficult, and introduces a risk of flashover across the contacts and to earth through the leakage of hot plasma. [3]

**Oil CB:** The oil CB employs the properties of the arc by using its energy to crack the oil molecules and generate gas, principally hydrogen, which with properly designed control systems can be used to sweep, cool and compress and arc plasma and so deionise it in a self extinguish process. [3]

**Sulphur Hexafluoride ( $\text{SF}_6$ ) CB:** Because of its electronegative attraction for electrons and its high ionisation energy,  $\text{SF}_6$  offers the possibility of working at much lower pressures or at much higher ratings per break than air. This type of CB passes high pressure  $\text{SF}_6$  through the interrupting nozzle to a low pressure region contained within the CB structure. [3]

**Vacuum CB:** The vacuum CB is one of the simplest judging by mechanical construction, consisting, in principle, of only a fixed and movable contact located in a vacuum vessel. When the contacts are separated, the arc is supported by ionised metal vapour derived from the contacts instead of by ionised gas as in other forms of interrupter, and at current zero collapse of ionisation and vapour condensation is very fast, ensuring interruption virtually independent of the rate of rise of restriking voltage. [3]

## 2.4 Switching Arc in a Circuit Breaker

As mentioned before, the electric arc created during the separation of the circuit breaker's contacts is indispensable in the process of current interruption. This electric arc behaves as a negative resistance, meaning its voltage decreases with the current, as shown in Figure 2.2 for direct current (DC). [7]

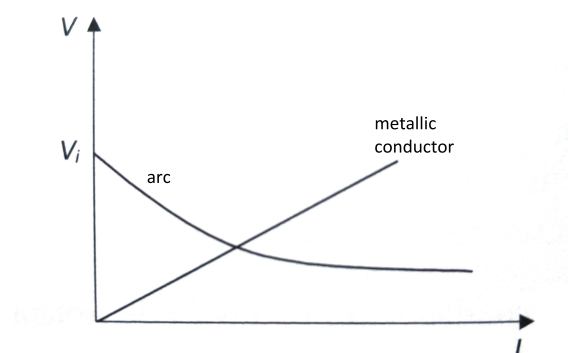


Figure 2.2: V/I characteristic of the electric arc in DC (adapted from [7])

### 2.4.1 Tripping the Circuit Breaker in Alternating Current

In contrast of direct current, where there is the need to create or force a current zero, in alternating current the value of the current passes through zero twice per cycle. Therefore, the zero condition is already fulfilled, and for the interruption to succeed it is only necessary to prevent the re-ignition of the arc after the current has passed zero. It is for this reason that de-ionization of the arc gap close to the time of a natural current zero is of utmost importance. [8]

This re-ignition is characterised by the current value not staying null after the supposed extinction of the arc occurred, as seen in Figure 2.3.

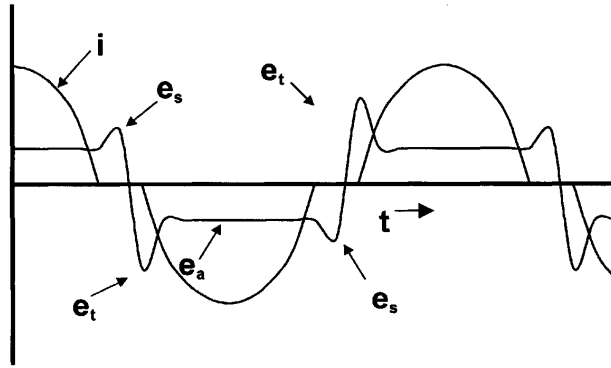


Figure 2.3: Typical variations of current and voltage showing the peak of extinction voltage  $e_s$  and peak of re-ignition voltage  $e_r$  [8]

In this figure,  $e_r$  represents the peak of re-ignition voltage,  $e_s$  represents the peak of extinction voltage,  $e_a$  is the arc voltage during the re-ignition and  $i$  is the current passing through the CB.

In case of a successful interruption, a similar phenomenon to the one shown in Figure 2.4 should occur.  $V$  and  $i$  are the grid's voltage and current (also referred as short-circuit current in this case),  $v_a$  is the arc voltage and  $v_r$  is the voltage between the terminals of the CB. [7]

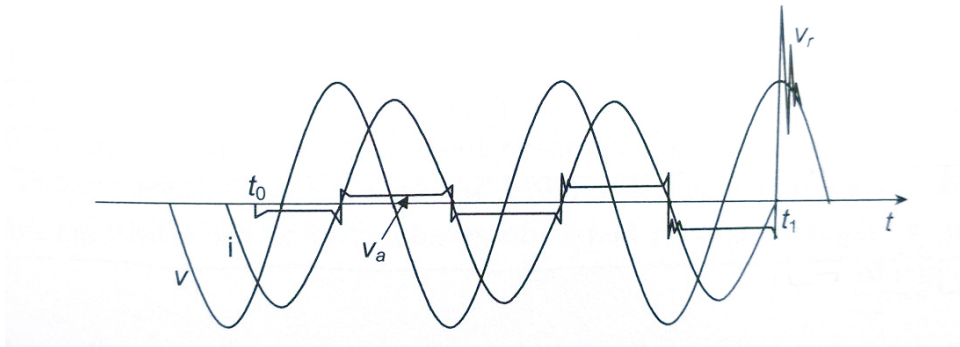


Figure 2.4: Grid voltage, short-circuit current, arc voltage and voltage measured between the circuit breaker terminals [7]

Analysing this figure, it can be concluded that the CB's contacts start to separate at  $t_0$ , establishing an arc between them. This voltage increases every cycle due to the increase in the separation until the distance between the contacts being too high, adding to the increased de-ionisation of the gap results in the extinction of the arc at  $t_1$ . Then, an oscillating period is established which originates a switching overvoltage. [7]

### 2.4.2 Transient Recovery Voltage in the opening of the Circuit Breaker

This oscillating period is also known as the Transient Recovery Voltage (TRV). This recovery voltage consists of two components, a transient component, occurring right after a current zero, and a steady-state component, which is the voltage that remains after the transient dies out. The actual waveform of the voltage oscillation however is determined by the parameters of the power system, normally being either a capacitive, inductive or resistive circuit. [9] The differences between each waveform are shown in Figure 2.5.

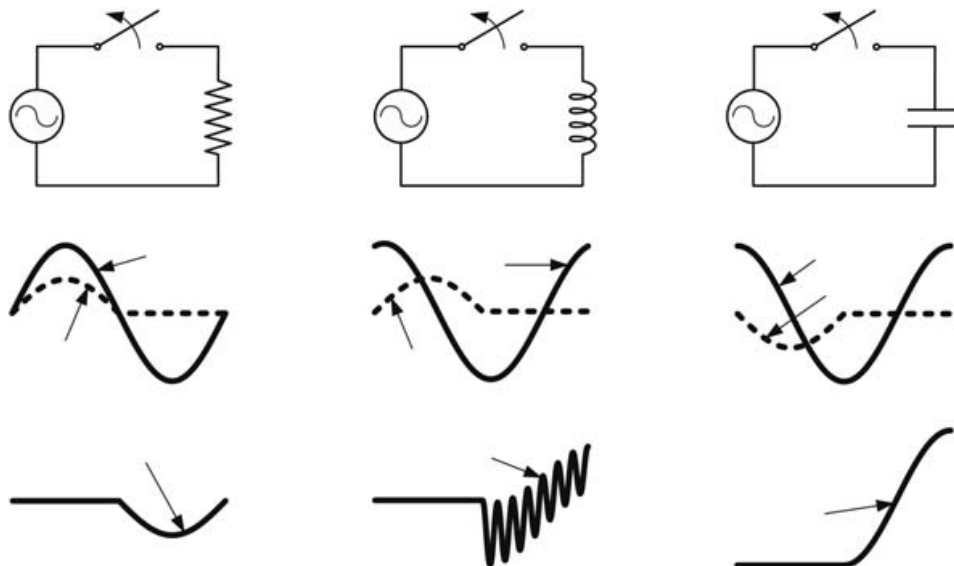


Figure 2.5: Transient Recovery Voltage of a resistive, inductive and capacitive circuit [9]

Another important factor in this oscillating phase is the Rate of Rise of Recovery Voltage (RRRV), which represents the peak transient recovery voltage divided by the total time from zero voltage to peak voltage. If the rate of recovery of the contact gap at the instant of current zero is faster than the RRRV, the interruption is successful. However, if the RRRV is faster than the recovery of the gap, then failure will occur and the probability of a re-ignition of the arc increases. [7,9]

Finally, as referred in [7–9], the moment where the current interruption is done is of great importance, as the switching overvoltage reaches much higher values when the interruption is not done near the moment of current zero. Figure 2.6 shows the difference in the TRV when the

interruption is done at the moment of current zero and at the moment of maximum current,  $v_r$  being the voltage between the terminals of the CB during the recovery process.

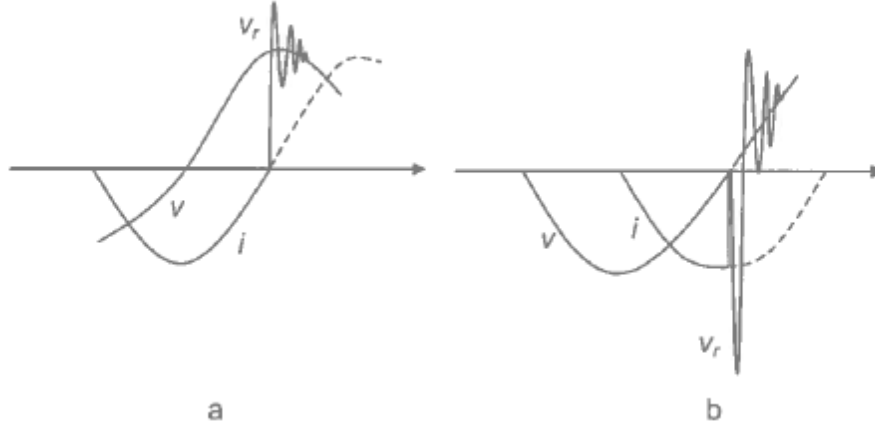


Figure 2.6: Transient Recovery Voltage: a) Current Zero; b) Max Current [7]

### 2.4.3 Mathematical Models used for modelling the Electric Arc

Over the years, the ability to correctly model the electric arc created during the opening of a circuit breaker gained a lot of importance in order to simulate its behaviour. Therefore, black box models were created to fulfill that necessity. A summary of these models and their functioning is explained in [10].

The two most relevant black box models for arc modelling and which were based on in many other models were described by O. Mayr [11] and A.M. Cassie [12], which will be explained in this section, along with a Mayr-type model developed in [13].

These models usually consist of one or two equations, all of them being a solution of the general arc equation: [14, 15]

$$\frac{d[\ln(g)]}{dt} = \frac{F'(Q)}{F(Q)} (P_{in} - P_{out}) \quad (2.1)$$

Where:

$$g = F(P_{in}, P_{out}, t) = \frac{i_{arc}}{u_{arc}} = \frac{1}{R} \quad (2.2)$$

Where:

$g$ : the momentary arc conductance

$P_{in}$ : the power supplied to the plasma channel

$P_{out}$ : the power transported from the plasma channel

$t$ : time

- $i_{arc}$  : the momentary arc current  
 $u_{arc}$ : the momentary arc voltage  
 $R$ : the momentary arc channel resistance  
 $Q$ : Energy constant per unit of volume

#### 2.4.3.1 Mayr's Arc Model [11]

The Mayr model describes the arc characteristic during zero-cross and can be used for arc-circuit interaction study. It is represented by the following equation:

$$\frac{1}{g_m} \frac{dg_m}{dt} = \frac{1}{\tau_m} \left( \frac{u_{arc} \cdot i_{arc}}{P_0} - 1 \right) \quad (2.3)$$

Where:

- $g_m$ : the arc conductance  
 $\tau_m$ : the arc time constant  
 $P_0$ : the cooling power constant  
 $u_{arc}$ : the arc voltage across the breaker  
 $i_{arc}$ : the arc current

#### 2.4.3.2 Cassie's Arc Model [12]

The Cassie model is well suited for studying the behaviour of the arc conductance in the high current zone. It can be summarised in the following equation:

$$\frac{1}{g_c} \frac{dg_c}{dt} = \frac{1}{\tau_c} \left( \frac{u_{arc}^2}{u_c^2} - 1 \right) \quad (2.4)$$

Where:

- $g_c$ : the arc conductance  
 $\tau_c$ : the arc time constant  
 $u_{arc}$ : the arc voltage across the breaker  
 $u_c$ : the arc voltage constant

However, this model is not suited for zero-cross studying, and should only be considered for its characteristic in the high current area.

#### 2.4.3.3 Schavemaker's Arc Model [13]

This model is an improvement of the Mayr model, complementing its flaw in the high current area. It takes the initial equation in 2.3 and adapts it in the following way:

$$\frac{1}{g} \frac{dg}{dt} = \frac{d \ln(g)}{dt} = \frac{1}{\tau} \left( \frac{u \cdot i}{\max(U_{arc}|i|, P_0 + P_1 u i)} - 1 \right) \quad (2.5)$$

Where:

- $g$ : the arc conductance

$\tau$ : the arc time constant

$P_0$ : the cooling power constant in Watt

$P_1$ : the cooling power constant which embodies the pressure built-up in the breaker caused by ohmic heating of the extinguishing medium by the arc

$u$ : the arc voltage across the breaker

$i$ : the arc current

$U_{arc}$ : the constant arc voltage in the high current area

With this equation, two different situations can be obtained. In the high current area, equation 2.5 reduces to the following:

$$\frac{1}{g} \frac{dg}{dt} = \frac{d \ln(g)}{dt} = \frac{1}{\tau} \left( \frac{u \cdot i}{U_{arc} |i|} - 1 \right) = \frac{1}{\tau} \left( \frac{u}{U_{arc}} - 1 \right) \quad (2.6)$$

Which is in conformity with the Cassie arc model [12], being valid in the high current area. At current zero, equation 2.5 reduces to the following:

$$\frac{1}{g} \frac{dg}{dt} = \frac{d \ln(g)}{dt} = \frac{1}{\tau} \left( \frac{u \cdot i}{P_0} - 1 \right) \quad (2.7)$$

It can be rapidly concluded that this equation is the same as 2.3, the Mayr arc model [11], which proves this model's validity in the current zero region.

This model uses both Cassie and Mayr's models to more accurately represent the arc from the high-current area to the zero-cross zone, being a useful tool for arc interaction study.

#### 2.4.3.4 PSCAD™/EMTDC™ implementation of the Arc Models

PSCAD™/EMTDC™ was used as the first simulation tool for this dissertation. Therefore, the mathematical arc models studied were first simulated in it to prove their efficiency and compare their behaviour. For this effect, an external library which simulated the behaviour of the electric arc during the CB opening was used, containing all three mathematical models studied [16].

The schematic used in this simulation is shown in Figure 2.7.

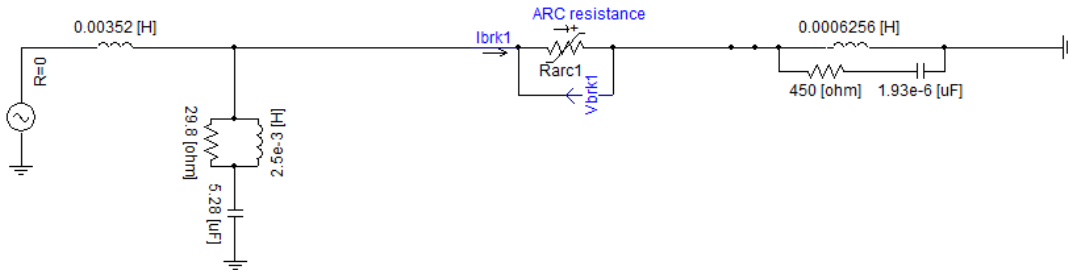


Figure 2.7: Schematic used to simulate the Circuit Breaker electric arc in PSCAD™/EMTDC™ [16]

The first RLC component is used to regulate the frequency at which the grid recovers after opening (TRV frequency) and the last RLC component simulates the load connected to the CB. In this case, its behaviour will be mainly inductive, as it is more similar to real situations. Finally,  $R_{arc1}$  represents the variable resistance inside the CB, controlled by an external object that, having the voltage and current measured between the terminals of the CB (in this case, the variable resistance) as inputs, implements the mathematical model desired starting at a specific time (controlled by the Timed Breaker Logic component seen in Figure 2.8) and outputs the calculated resistance.

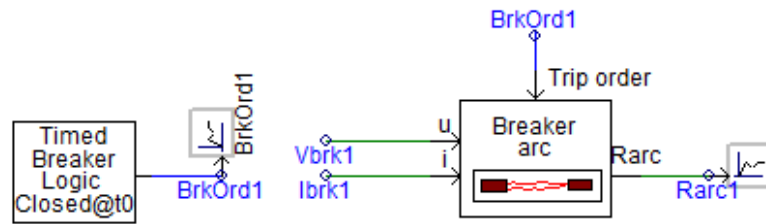


Figure 2.8: External object used to simulate the Mayr, Cassie and Schavemaker arc models' behaviour [16]

The first model to be tested was the Mayr's Arc Model. In it, the values chosen for the  $\tau_m$  and  $P_0$  constants were  $0.3\mu s$  and  $32.9\text{ kW}$ , respectively, as seen in Figure 2.9.

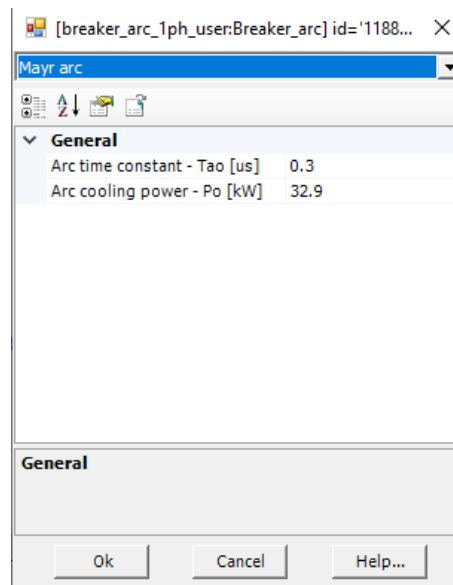


Figure 2.9: Values used for the constants in the Mayr Arc Model implementation

This produced the results shown in Figure 2.10 and 2.11. With them, it can be concluded, as mentioned in 2.4.3.1, that this model gives a good representation of the zero-cross arc characteristic. However, it does not give a good representation of arc behaviour in the high current area (before zero-cross).

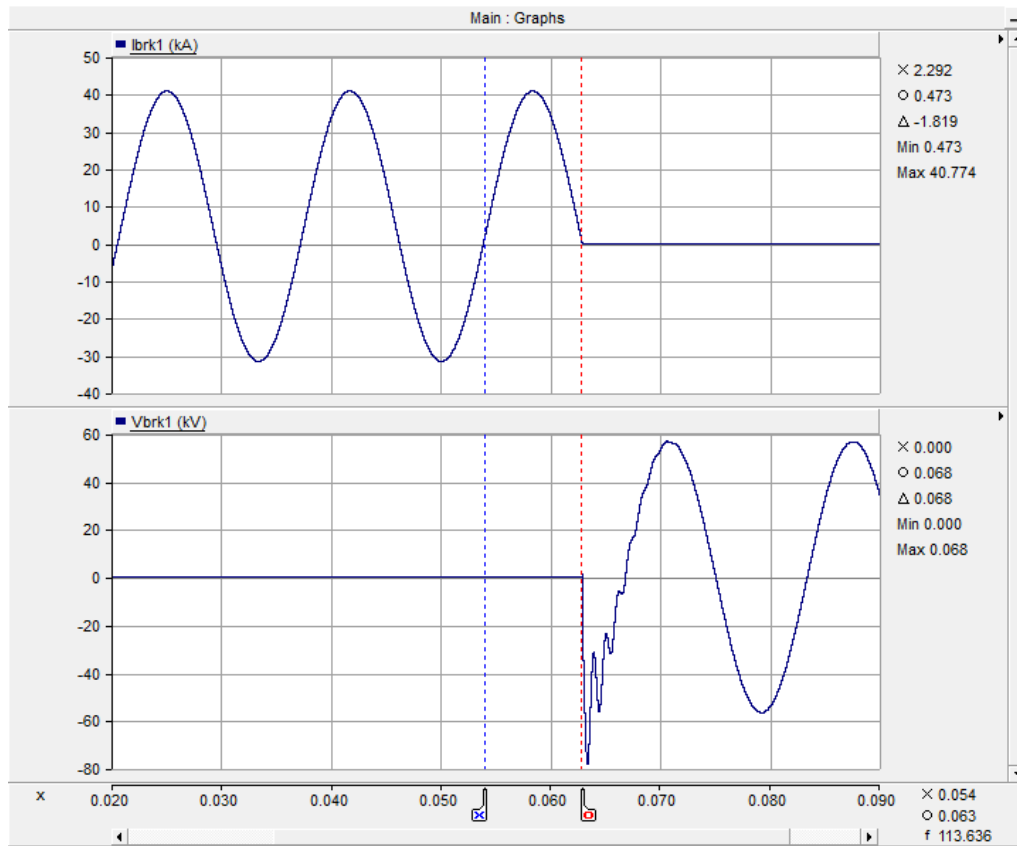


Figure 2.10: Current and Voltage obtained in the Mayr Arc Model Simulation

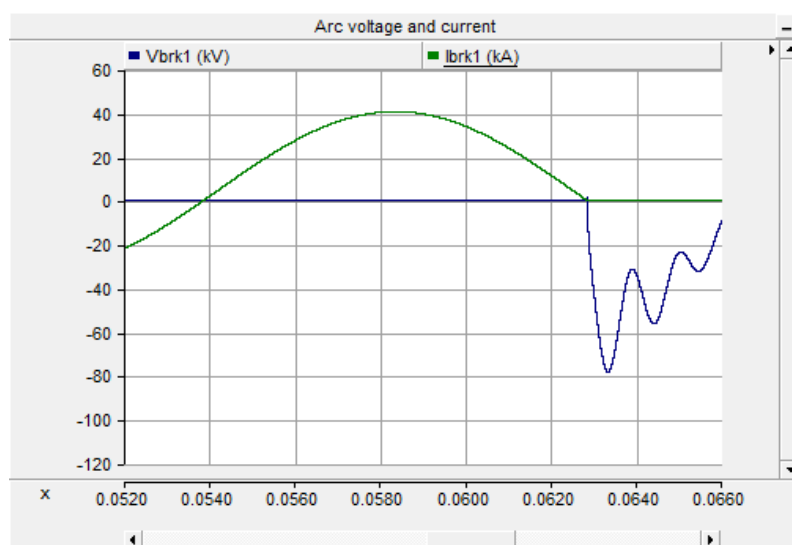


Figure 2.11: Mayr simulation's Voltage and Current in the moment of Circuit Breaker opening



After Mayr's model, Cassie's Arc Model was tested. The parameters chosen are seen in Figure 2.12,  $\tau_c$  taking the value of  $0.6 \mu s$  and the Arc voltage constant  $U_c$  was input as 3.85 kV.

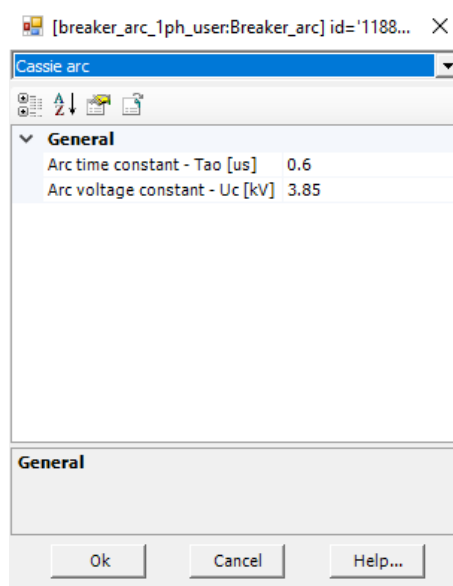


Figure 2.12: Values used for the constants in the Cassie Arc Model implementation

With these parameters, the following waveforms represented in Figures 2.13 and 2.14 were obtained. By observing them, it can be easily concluded that this model can only be used for its characteristic in the high current area, as it does not give a accurate representation of arc behaviour during zero-cross.

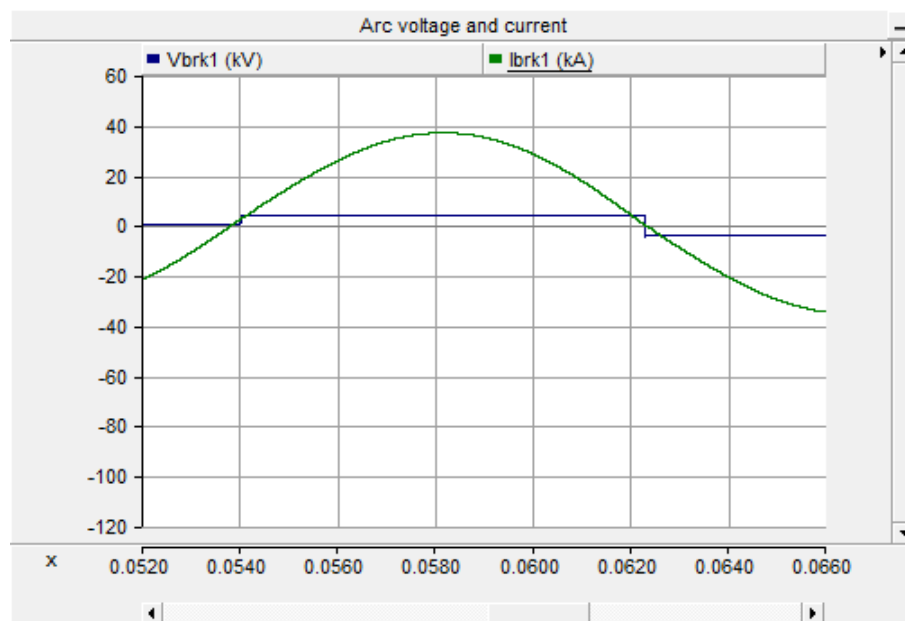


Figure 2.13: Cassie simulation's Voltage and Current in the moment of Circuit Breaker opening

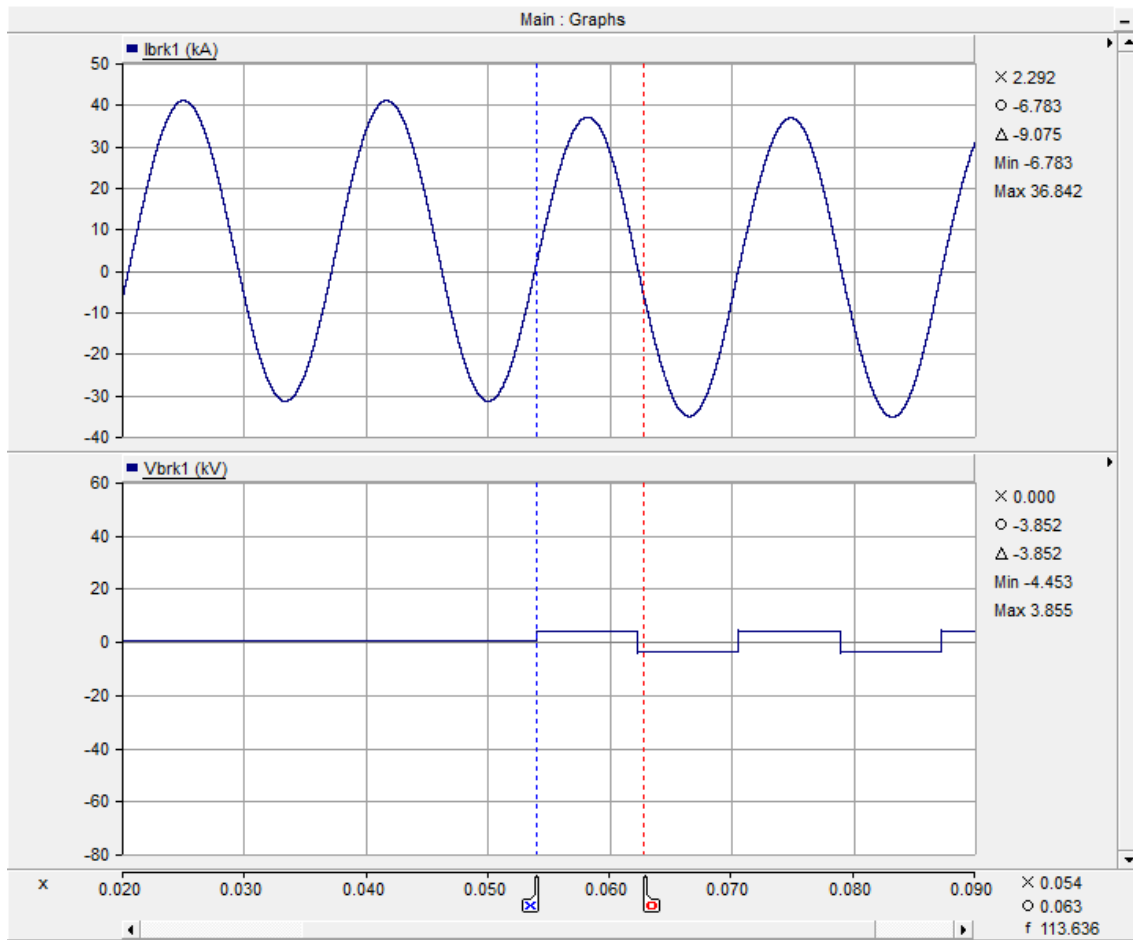


Figure 2.14: Current and Voltage obtained in the Cassie Arc Model Simulation

Finally, the Schavemaker's Arc Model was implemented. The values for the parameters can be seen in Figure 2.15, them being:  $\tau = 0.27 \mu\text{s}$ ;  $P_0 = 15917 \text{ W}$ ;  $P_1 = 0.9943 \text{ pu}$ ;  $U_{arc} = 1.1 \text{ kV}$ .

Using these inputs, as in the other two cases, the following waveforms for voltage and current were obtained, as seen in Figures 2.16 and 2.17. In contrary to the other two models mentioned before, the Schavemaker Model brings an accurate representation of zero-cross arc interaction while having a decent representation in the high current area. However, its high current area representation has some flaws, as explained in [17], but it is accurate enough to correctly model the electric arc during the CB opening for analysis and studying.

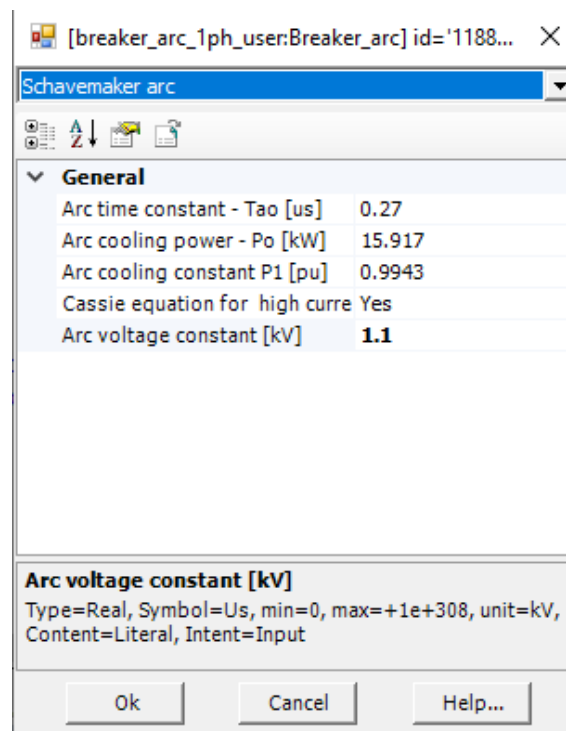


Figure 2.15: Values used for the constants in the Schavemaker Arc Model implementation

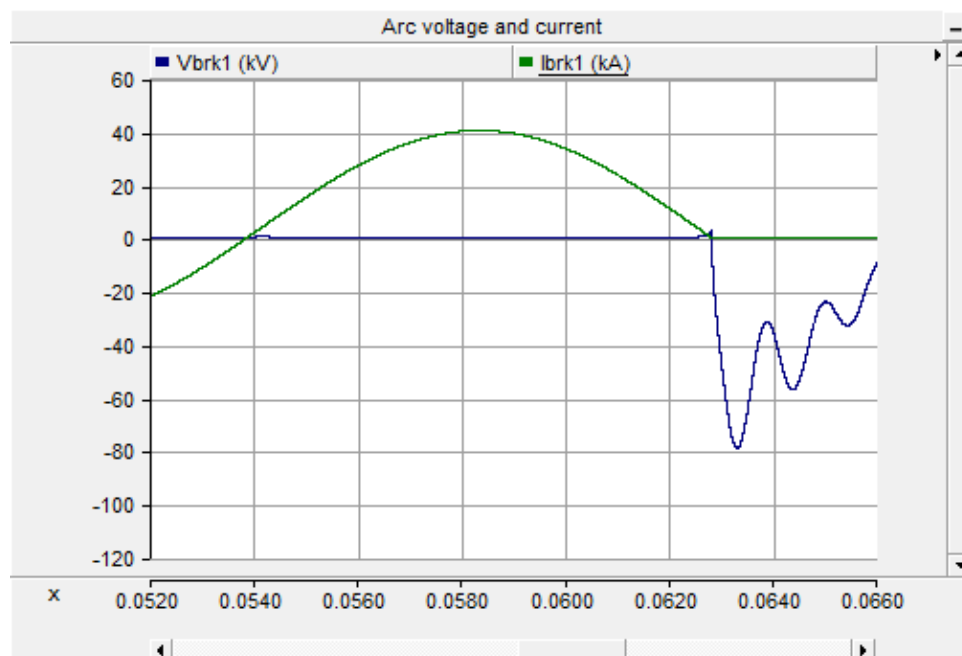


Figure 2.16: Schavemaker simulation's Voltage and Current in the moment of Circuit Breaker opening

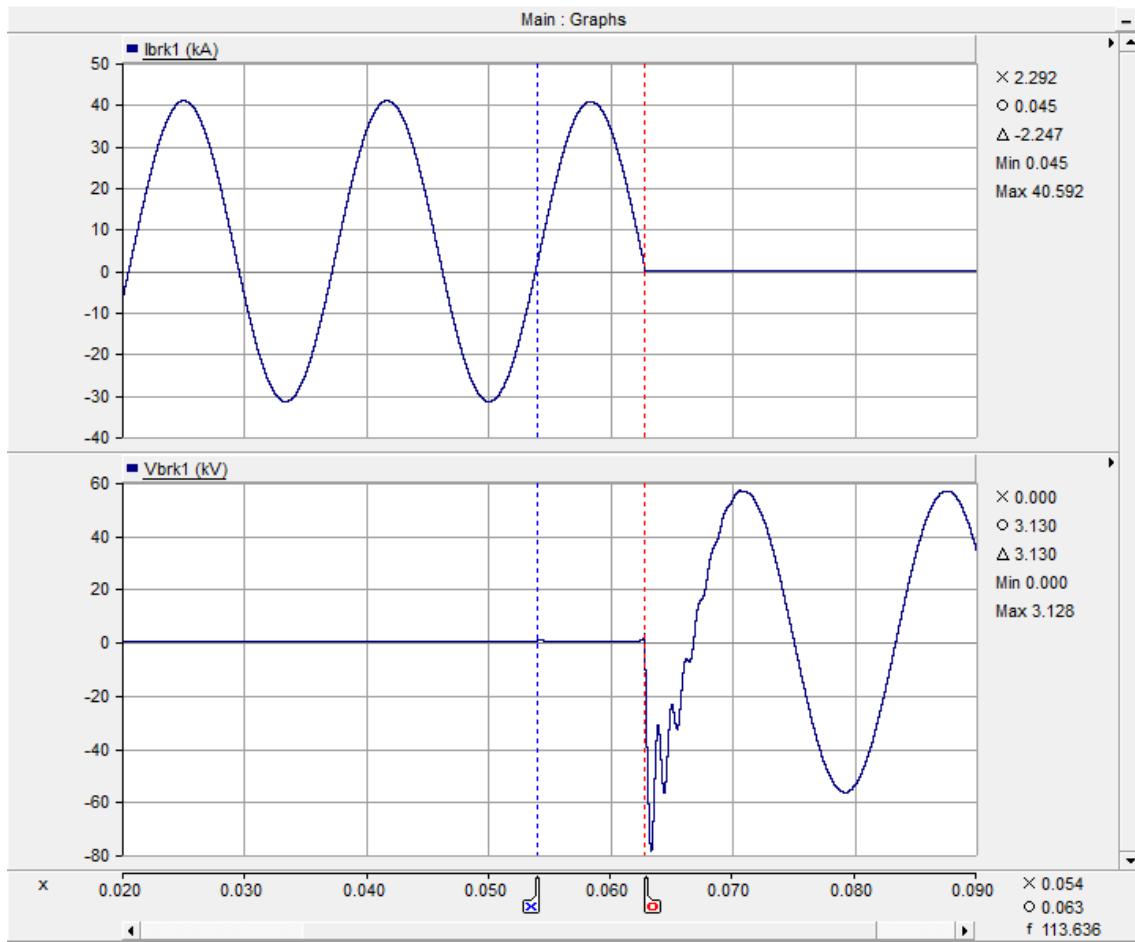


Figure 2.17: Current and Voltage obtained in the Schavemaker Arc Model Simulation

## 2.5 Summary

In this chapter, a CB's design and functioning were presented, together with the electric arc behaviour during an opening operation. In addition to that, Mayr, Cassie and Schavemaker's electric arc models were addressed and their benefits and flaws were concluded through simulating each one and analysing the results.

Although these were the three models being explained, many others models such as the KEMA model [18], the Habedank model [19], the model described in [17] which proposes an arc model before current zero, the hybrid Cassie-Mayr arc model presented in [20] or many others used as bases/references for these models are useful for arc interaction studies since they can accurately represent the arc in the areas they are meant to.

With all this considered, and since PSCAD<sup>TM</sup>/EMTDC<sup>TM</sup> was used as the initial simulation tool and contained the external library implementing the Cassie, Mayr and Schavemaker arc models shown in this section, the Schavemaker model will be the one used for arc interaction study in this work.

## Chapter 3

# IEC 61850 based disturbance and fault recorder for Electric Arc Modelling in Circuit Breakers

In this chapter, the standards which helped merge all the different approaches taken until then regarding data transmission in substations are mentioned. More specifically, the IEC 61850 standard is explained, detailing its role in the modelling and functioning of an IED inside a substation, and the COMTRADE standard is addressed to understand how the information from an IED can be used to determine the condition of the different equipments inside a substation.

### 3.1 Substation Automation Systems and IEC 61850

Following the evolution of the technologies available to use, conventional control and monitoring panels in the substation have been replaced by the Substation Automation Systems (SAS) [21]. Another factor that has impacted the evolution of the substation systems is the increasing demand in the electrical grid. While the demands on the grid have continued to increase, additional investments in it have not always matched the requirements [22].

In order to take advantage of modern technology to deliver additional new benefits to users of substation automation, the International Electrotechnical Commission (IEC) developed and released a new global standard for substation automation: IEC 61850 [23]. As defined in the IEC 61850 standard, the SAS are divided in three major levels, as shown in figure 3.1.

The first level, the process level, refers to the power system equipment in the substation represented by the process interface. The bay level consists of bay protection and control IEDs hosting the related functions. Finally, the station level refers to tasks for the complete substation and consists typically of the substation computer with central functions and human-machine interface (HMI) and of the gateway to the network control center [24]. In addition to that, the process level should be separated into two parts independently, i.e. SV network and GOOSE network.

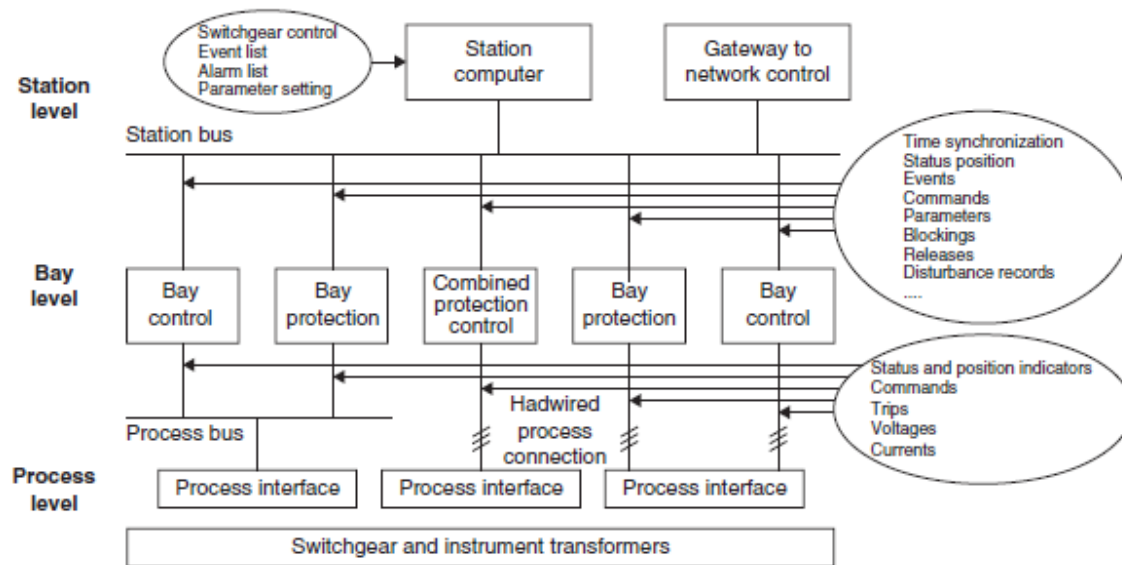


Figure 3.1: Configuration of substation automation system and data exchange [24]

This configuration referred to as the “Three-layers and Two-networks” has been proven to be good for the safety and stability of the substation [25].

### 3.1.1 IEC 61850 System Configuration Description Language

IEC 61850-6 specifies a file format for describing communication-related IED configurations and IED parameters, communication system configurations, switch yard (function) structures, and the relations between them. The main purpose of this format is to exchange IED capability descriptions, and SAS descriptions between IED engineering tools and the system engineering tool(s) of different manufacturers in a compatible way. This defined language is called System Configuration description Language (SCL) [26].

#### 3.1.1.1 Models Described by SCL

SCL describes the following object models: (i) The primary system structure which describes the primary apparatus functions used and how the apparatus are connected; (ii) The communication system which describes how IEDs are connected to subnetworks and networks; (iii) The application level communication which describes how data is grouped into data sets for sending and how IEDs trigger the sending process as well as the service chosen and the input data needed; (iv) Each IED which contains logical devices, logical nodes (LNs), reports, data contents, available associations and data; (v) Instantiable LN type definitions; (vi) The relations between LNs, their hosting IEDs and the switchyard parts [26, 27].

### 3.1.1.2 Structure of a SCL File

A typical SCL file is divided into 5 elements: (i) The **Header**, which is used to identify an SCL configuration file and its version, while also specifying options for the mapping of names to signals; (ii) The **Substation**, to describe the functional structure of a substation and identify the primary devices and their electrical connections; (iii) The **IED** describes the pre-configuration of an IED, its access points, the logical devices and LNs instantiated on it; (iv) The **Communication**, describing the direct communication possibilities between LNs by means of logical (SubNetworks) buses and IED access points (ConnectedAP); (v) The **DataTypeTemplates** defines instantiable LN types including an instantiable LN type (LNType), an instantiable DATA type (DOType), an instantiable structured attribute type (DAType), and an enumeration type (EnumType) [26–28].

Figure 3.2 shows the typical structure of a SCL configuration file.

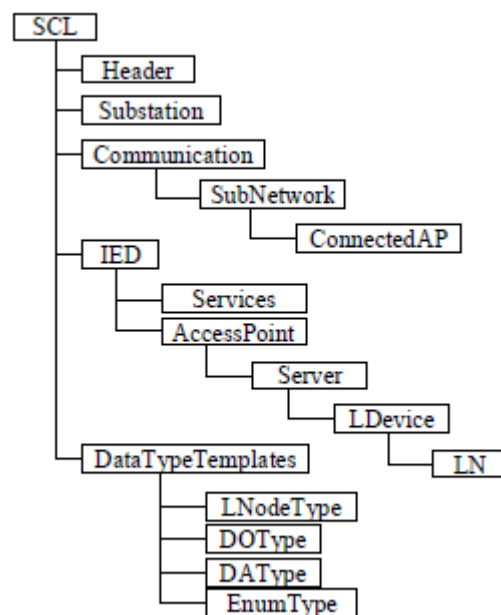


Figure 3.2: Structure of a SCL configuration file [28]

### 3.1.1.3 SCL File Types

The first edition of IEC 61850-6 specifies four types of SCL files: (i) **Configured IED Description** (CID), used when data is exchanged from IED configuration tool to IED. It describes an instantiated IED within an engineering project; (ii) **IED Capability Description** (ICD), used when data is exchanged from IED configuration tool to system configuration tool, and describes the capabilities of an IED. Generally this file is preconfigured when IEDs leave factory. It should contain the elements Header, IED and DataTypeTemplates; (iii) **System/Substation Specification Description** (SSD), used when data is exchanged from a system specification tool to the system configuration tool. It describes the single line diagram of the substation and the required LNs. The file

contains a substation description section, the needed data type templates and LN type definitions. (iv) **Substation Configuration Description** (SCD), used when data is exchanged from a system configuration tool to an IED configuration tool. It contains all IEDs, a communication configuration section and a substation description section [27]. Additionally, two new types of new SCL files were proposed in the second edition of IEC 61850-6: **Instantiated IED Description** (IID) and **System-exchange Description** (SED), to deal with IED modification after configuration and exchange of configuration data between different projects, respectively [29].

A schematic diagram of a substation engineering process with these SCL files is shown in figure 3.3.

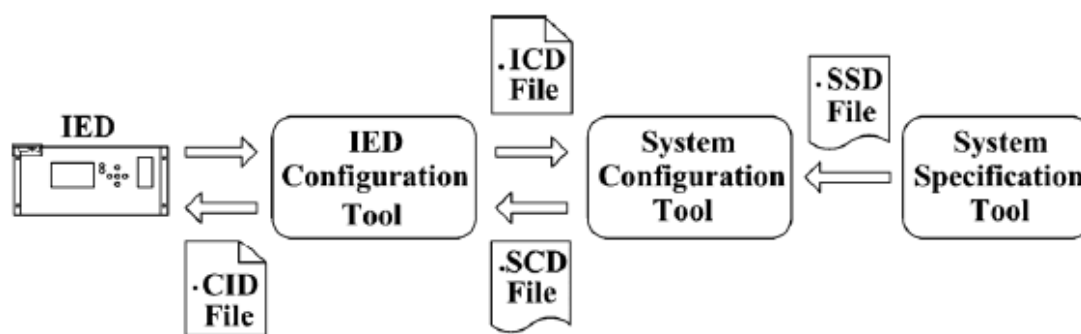


Figure 3.3: Substation engineering process with SCL files [29]

#### 3.1.1.4 Advantages from IEC 61850-6

All things considered, it is visible that the standardization of communication protocols in substations brought by the IEC 61850 standard is a improvement to the conventional engineering process, which were mostly proprietary solutions. Being closed systems relying on highly specialised hardware and vendor-specific software, they had a number of problems and limitations [30].

Specifically for IEDs and the IEC 61850-6 standard in particular, this standardization allows the development of universal IED setting tools and significantly simplifies their configuration process [31].

### 3.1.2 IEC 61850 Basic Information and Communication Structure

IEC 61850-7 describes an abstract communication service interface (ACSI), and the generic functions (called LNs) descriptions which are defined by reusing common data classes.

#### 3.1.2.1 IEC 61850 Part 7-1: Principles and models [32]

The purpose of this part of the IEC 61850 series is to help understand the basic modelling concepts and description methods for substation-specific information models for power utility automation



systems, device functions used for power utility automation purposes and communication systems to provide interoperability within power utility facilities.

In addition to that, it also provides explanations and detailed requirements relating to the relation between IEC 61850-7-4, IEC 61850-7-3, IEC 61850-7-2 and IEC 61850-5. The way how the abstract services and models of the IEC 61850-7-x series are mapped to concrete communication protocols as defined in IEC 61850-8-1 is also detailed in this part.

### 3.1.2.2 IEC 61850 Part 7-2: Abstract communication service interface (ACSI) [33]

This document applies to the ACSI communication for utility automation. The ACSI provides interfaces for the following abstract communication services: **a)** Abstract interface describing communications between a client and a remote server for real-time data access and retrieval, device control, event reporting and logging, setting group control, self-description of devices (device data dictionary), data typing and discovery of data types, and file transfer; **b)** Abstract interface for fast and reliable system-wide event distribution between an application in one device and many remote applications in different devices (publisher/subscriber) and for transmission of sampled measured values (publisher/subscriber).

Figures 3.4 and 3.5 show an example of an ACSI server building block and ACSI's communication model, respectively [34].

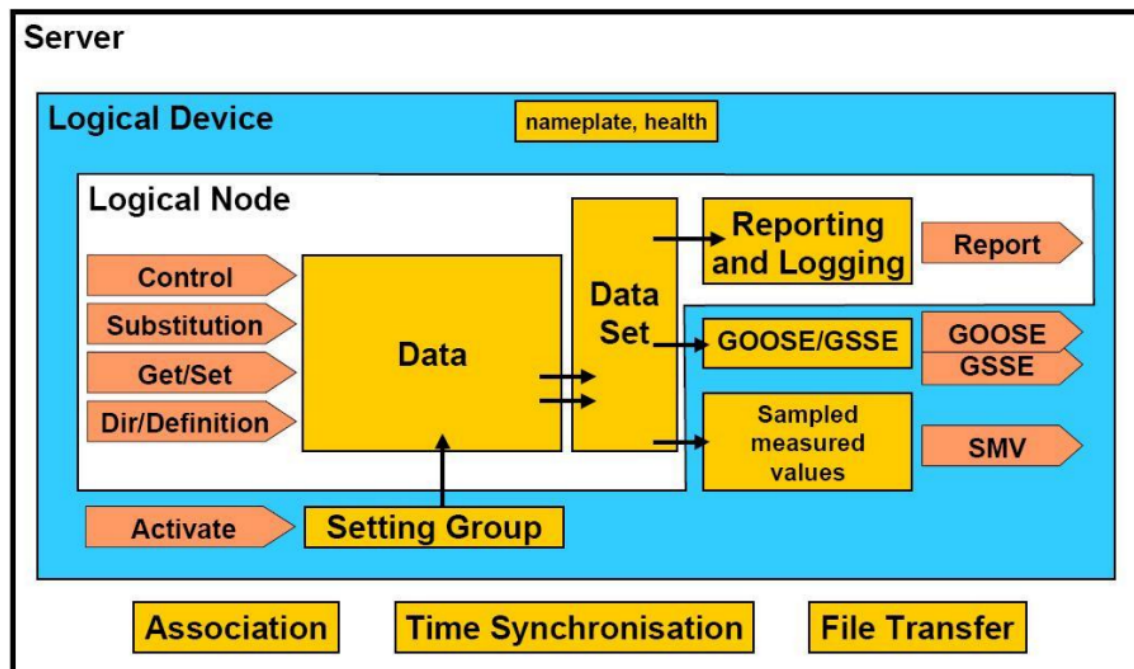


Figure 3.4: ACSI server building block [34]

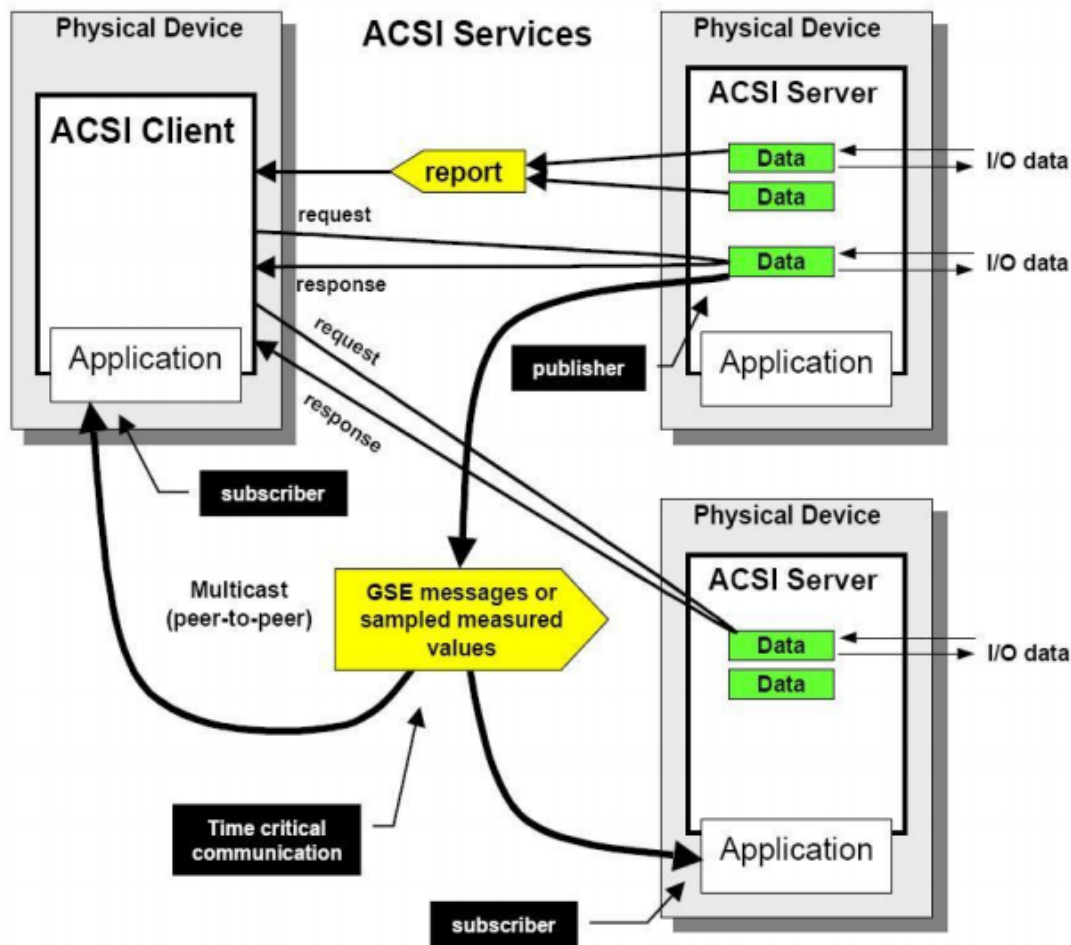


Figure 3.5: ACSI communication model [34]

### 3.1.2.3 IEC 61850 Part 7-3: Common Data Classes [35]

This part of IEC 61850 specifies constructed attribute classes and common data classes (CDC) related to substation applications. In particular, it specifies CDC for status information, measured information, control, status settings, analogue settings and attribute types used in these CDC. It is applicable to the description of device models and functions of substations and feeder equipment.

In addition to that, it may also be applied, for example, to describe device models and functions for substation to substation information exchange, substation to control centre information exchange, power plant to control centre information exchange, information exchange for distributed generation, or information exchange for metering.

Figure 3.6 shows an example of a Single Point Status (SPS) class.

#### 3.1.2.4 IEC 61850 Part 7-4: Compatible logical node classes and data object classes [36]

Finally, part 7-4 of the IEC 61850 Standard specifies the information model of devices and functions generally related to common use regarding applications in systems for power utility au-

SPS class					
Data attribute name	Type	FC	TrgOp	Value/Value range	M/O/C
<b>status</b>					
stVal	BOOLEAN	ST	dchg	TRUE   FALSE	M
q	Quality	ST	qchg		M
t	TimeStamp	ST			M
<b>substitution and blocked</b>					
subEna	BOOLEAN	SV			PICS_SUBST
subVal	BOOLEAN	SV		TRUE   FALSE	PICS_SUBST
subQ	Quality	SV			PICS_SUBST
subID	VISIBLE STRING64	SV			PICS_SUBST
blkEna	BOOLEAN	BL			O
<b>configuration, description and extension</b>					
d	VISIBLE STRING255	DC		Text	O
dU	UNICODE STRING255	DC			O
cdcNs	VISIBLE STRING255	EX			AC_DLND_A_M
cdcName	VISIBLE STRING255	EX			AC_DLND_A_M
dataNs	VISIBLE STRING255	EX			AC_DLN_M

Figure 3.6: SPS class

tomation. It also contains the information model of devices and function-related applications in substations. In particular, it specifies the compatible LN names and data object names for communication between IED's. This includes the relationship between LNs and data objects.

Figure 3.7 exemplifies a definition of a CB LN, which is used for modelling switches with short-circuit breaking capabilities, and adding to other LNs can complete the logical modelling for the breaker being represented. Figure 3.8 shows an example of a data object definition, which in this case represents the physical capabilities of the operating breaker.

XCBR class				
Data object name	Common data class	Explanation	T	M/O/C
<b>Descriptions</b>				
EEName	DPL	External equipment name plate		O
<b>Status information</b>				
EEHealth	ENS	External equipment health		O
LocKey	SPS	Local or remote key (local means without substation automation communication, hardwired direct control)		O
Loc	SPS	Local control behaviour		M
OpCnt	INS	Operation counter		M
CBOPCap	ENS	Circuit breaker operating capability		O
POWCap	ENS	Point on wave switching capability		O
MaxOpCap	INS	Circuit breaker operating capability when fully charged		O
Dsc	SPS	Discrepancy		O
<b>Measured and metered values</b>				
SumSwARs	BCR	Sum of switched amperes, resettable		O
<b>Controls</b>				
LocSta	SPC	Switching authority at station level		O
Pos	DPC	Switch position		M
BlkOpn	SPC	Block opening		M
BlkCls	SPC	Block closing		M
ChaMotEna	SPC	Charger motor enabled		O
<b>Settings</b>				
CBTms	ING	Closing time of breaker		O

Figure 3.7: Circuit Breaker Logical Node Definition

Breaker operating capability	Value
None	1
Open	2
Close – Open	3
Open – Close – Open	4
Close – Open – Close – Open	5
Open – Close – Open – Close – Open	6
more	7

Figure 3.8: Data Object Definition for a Circuit Breaker operating capability

## 3.2 Common format for Transient Data Exchange for power systems (COMTRADE)

COMTRADE was developed by the IEEE Power and Energy Society Power System Relaying Committee, defining a common format for data exchange between various sources and facilitating systems to use digital data from other systems. More specifically, fault and transient data analysis benefit the most from this standard, allowing various devices to use the data provided to enhance and automate the analysis, testing, evaluation, and simulation of power systems and related protection schemes during fault and disturbance condition [37].

### 3.2.1 COMTRADE File Types [38]

The COMTRADE standard defines four types of files associated with every record set, each one of them carrying a different class of information. In the same set, all files must have the same name, only changing the extension indicating the type of file.

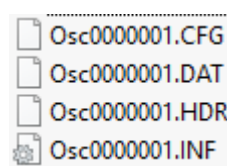


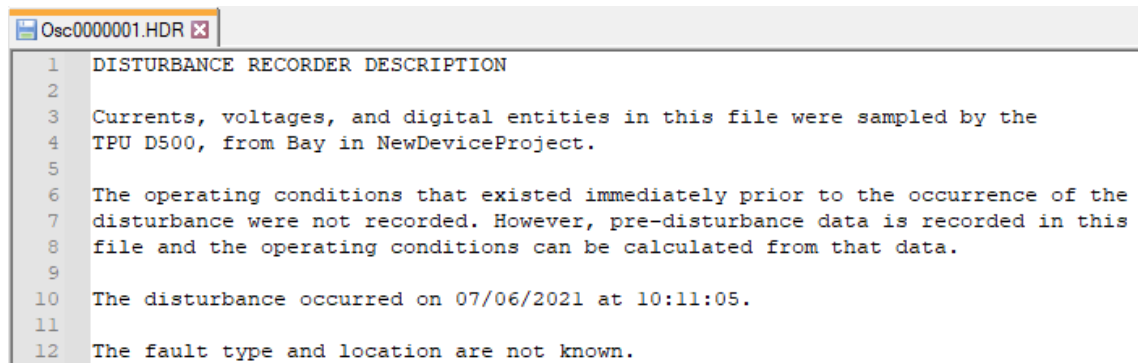
Figure 3.9: Record set with all four different file types

In the set shown in Figure 3.9, it can be seen that the COMTRADE files follow the format xxxxxxxx.yyy, where the xxxxxxxx part represents the set name, in this case Osc0000001, and the yyy part represents the file type, using the extensions .CFG for a config file, .DAT for a data file, .HDR for a header file and .INF for an information file.

#### 3.2.1.1 Header File (.HDR)

The header file is an optional ASCII text file created by the originator of the COMTRADE data, typically through the use of a word processor program, being intended to be printed and read by

the user. The header file format is ASCII, and in it the creator of the header file can include any information in any order desired.



```

1 DISTURBANCE RECORDER DESCRIPTION
2
3 Currents, voltages, and digital entities in this file were sampled by the
4 TPU D500, from Bay in NewDeviceProject.
5
6 The operating conditions that existed immediately prior to the occurrence of the
7 disturbance were not recorded. However, pre-disturbance data is recorded in this
8 file and the operating conditions can be calculated from that data.
9
10 The disturbance occurred on 07/06/2021 at 10:11:05.
11
12 The fault type and location are not known.

```

Figure 3.10: Header file example

Figure 3.10 was obtained from a recording during this dissertation, providing information about the disturbance recorded, meant to be read by the user who opens the file.

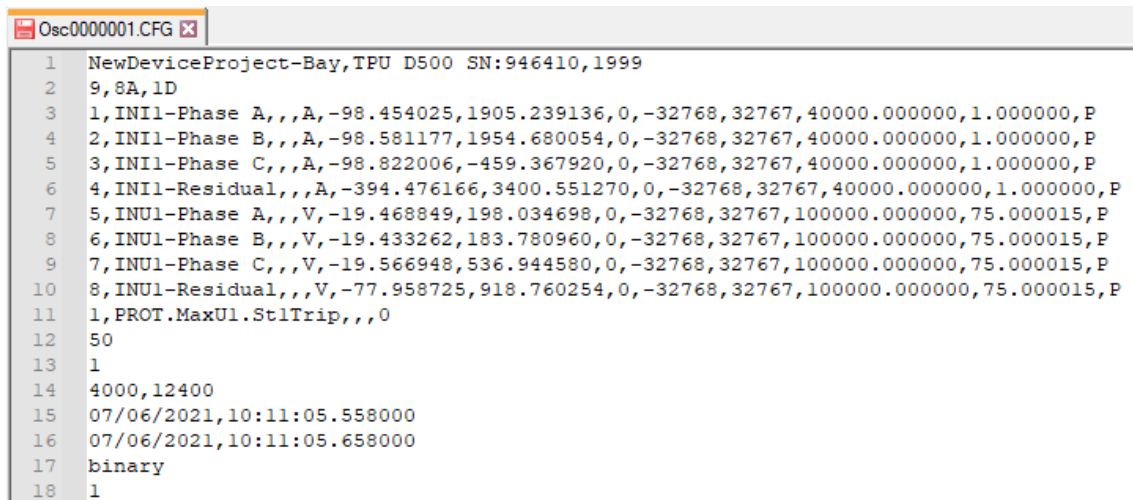
### 3.2.1.2 Configuration File (.CFG)

The configuration file is an ASCII text file intended to be read by a computer program and, therefore, must be saved in a specific format. The configuration file contains information needed by a computer program in order to properly interpret the data (.DAT) file. This information includes items such as sample rates, number of channels, line frequency, channel information, etc.

The configuration file shall have the following information:

- a) Station name, identification of the recording device, and COMTRADE Standard revision year (if the year is not present, the 1991 original issue date is assumed);
- b) Number and type of channels;
- c) Channel names, units, and conversion factors;
- d) Line frequency;
- e) Sample rate(s) and number of samples at each rate;
- f) Date and time of first data point;
- g) Date and time of trigger point;
- h) Data file type;
- i) Time Stamp Multiplication Factor.

The configuration file can be created with a word processing program or by a computer program that creates the configuration file from the data that is the source of the transient record. If a word processor is used to create the configuration file, it must save the data in ASCII text file format.



```

1 NewDeviceProject-Bay,TPU D500 SN:946410,1999
2 9,8A,1D
3 1,INI1-Phase A,,,A,-98.454025,1905.239136,0,-32768,32767,40000.000000,1.000000,P
4 2,INI1-Phase B,,,A,-98.581177,1954.680054,0,-32768,32767,40000.000000,1.000000,P
5 3,INI1-Phase C,,,A,-98.822006,-459.367920,0,-32768,32767,40000.000000,1.000000,P
6 4,INI1-Residual,,,A,-394.476166,3400.551270,0,-32768,32767,40000.000000,1.000000,P
7 5,INU1-Phase A,,,V,-19.468849,198.034698,0,-32768,32767,100000.000000,75.000015,P
8 6,INU1-Phase B,,,V,-19.433262,183.780960,0,-32768,32767,100000.000000,75.000015,P
9 7,INU1-Phase C,,,V,-19.566948,536.944580,0,-32768,32767,100000.000000,75.000015,P
10 8,INU1-Residual,,,V,-77.958725,918.760254,0,-32768,32767,100000.000000,75.000015,P
11 1,PROT.MaxUl.StlTrip,,,0
12 50
13 1
14 4000,12400
15 07/06/2021,10:11:05.558000
16 07/06/2021,10:11:05.658000
17 binary
18 1

```

Figure 3.11: Configuration file example

In Figure 3.11, the information as defined by the standard is visible, being divided in lines (each line ends with a <CR/LF> command). It also contains a field that identifies whether the companion data file is stored in ASCII or binary format. This is of extreme importance when processing the recording data, as the data processor must know which format is being used for correct interpretation.

### 3.2.1.3 Data File (.DAT)

The data file contains the value for each input channel for each sample in the record. The number stored for a sample is a scaled version of the value presented to the device that sampled the input waveform. The stored data may be either zero-based or it may have a zero offset. Zero-based data spans from a negative number to a positive number (e.g., -2000 to 2000). Zero-offset numbers are all positive with a positive number chosen to represent zero (e.g., 0 to 4000, with 2000 representing zero). Conversion factors specified in the configuration file define how to convert the data values to engineering units. The data file also contains a sequence number and time stamp for each set of samples. In addition to data representing analog inputs, digital inputs are also frequently recorded. In this standard, this type of input is referred to as a status input. The state of a status input is represented by a number "1" or "0" in the data file. The data files may be in either ASCII or binary format, explicit in a field in the corresponding configuration file.

**ASCII Data Files** The ASCII data file is divided into rows and columns. The number of data rows varies with the length of the recording and affects the length of the file. Each row shall

be divided into  $X+2$  columns where  $X$  is the total number of channels, analog and status, in the recording; and the other two are for the sample number and time stamp. The number of columns is dependent upon the recording system and also affects the file length. Field lengths specified for ASCII data files are maximum values and are not fixed lengths. All numeric characters, including sign notation, shall fit within the field length limits.

- a) The first column contains the sample number.
- b) The second column is the time stamp for the data of that sample number.
- c) The third set of columns contain the data values that represent analog information.
- d) The fourth set of columns contain the data for the status channels. If all the columns containing data values do not fit on the same line, they are continued without a carriage return/line feed (<CR/LF>) until all data values for that sample have been displayed. The last value shall be terminated with carriage return/line feed (<CR/LF>).
- e) The next row (line) begins with the next sample number followed by the next data set.
- f) An ASCII end of file (EOF) marker ("1A" HEX) is placed immediately following the carriage return/line feed (<CR/LF>) of the last data row of the file.

Each data sample record consists of integers arranged as follows:

**n, timestamp,  $A_1, A_2, \dots, A_k, D_1, D_2, \dots, D_m$**

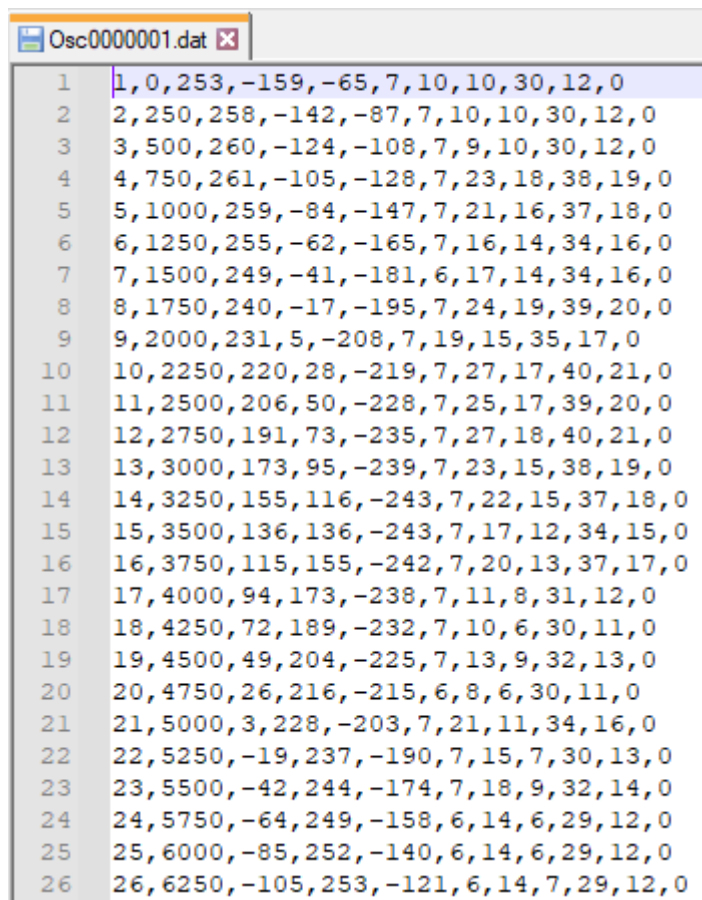
Where  $n$  is the sample number, timestamp is the time stamp,  $A_1 \dots A_k$  are the analog channel data values and  $D_1 \dots D_m$  are the status channel data values.

Figure 3.12 exemplifies a data file in ASCII format.

**Binary Data Files** The binary data files use the same basic structure as the one used for the ASCII data files, with the exception that status channel data are compacted as described below. The format is sample number, time stamp, data value for each analog channel, and grouped status channel data for each sample in the file. The data within a binary sample record is not separated by commas and the end of a sample record is not marked by carriage return/line feed characters, since a binary data file is a continuous stream of binary data. Data translation is determined by sequential position within the file, and if any data element is missing or corrupt, the sequence of variables is lost and the file may be unusable.

Data is stored in binary format, but for convenience the values are shown in hexadecimal here. When storing a two-byte (16 bit) word, the standard DOS format is to store the least significant byte (LSB) of the data first, then the most significant byte (MSB). The two-byte data value "1234" will be stored in "3412" format. In storing a four-byte (32 bit) word, the least significant byte (LSB) of the word is stored first, then the next to least significant byte, then the next to most significant byte, then the most significant byte (MSB). The four-byte data value "12345678" will





Line	Data
1	1, 0, 253, -159, -65, 7, 10, 10, 30, 12, 0
2	2, 250, 258, -142, -87, 7, 10, 10, 30, 12, 0
3	3, 500, 260, -124, -108, 7, 9, 10, 30, 12, 0
4	4, 750, 261, -105, -128, 7, 23, 18, 38, 19, 0
5	5, 1000, 259, -84, -147, 7, 21, 16, 37, 18, 0
6	6, 1250, 255, -62, -165, 7, 16, 14, 34, 16, 0
7	7, 1500, 249, -41, -181, 6, 17, 14, 34, 16, 0
8	8, 1750, 240, -17, -195, 7, 24, 19, 39, 20, 0
9	9, 2000, 231, 5, -208, 7, 19, 15, 35, 17, 0
10	10, 2250, 220, 28, -219, 7, 27, 17, 40, 21, 0
11	11, 2500, 206, 50, -228, 7, 25, 17, 39, 20, 0
12	12, 2750, 191, 73, -235, 7, 27, 18, 40, 21, 0
13	13, 3000, 173, 95, -239, 7, 23, 15, 38, 19, 0
14	14, 3250, 155, 116, -243, 7, 22, 15, 37, 18, 0
15	15, 3500, 136, 136, -243, 7, 17, 12, 34, 15, 0
16	16, 3750, 115, 155, -242, 7, 20, 13, 37, 17, 0
17	17, 4000, 94, 173, -238, 7, 11, 8, 31, 12, 0
18	18, 4250, 72, 189, -232, 7, 10, 6, 30, 11, 0
19	19, 4500, 49, 204, -225, 7, 13, 9, 32, 13, 0
20	20, 4750, 26, 216, -215, 6, 8, 6, 30, 11, 0
21	21, 5000, 3, 228, -203, 7, 21, 11, 34, 16, 0
22	22, 5250, -19, 237, -190, 7, 15, 7, 30, 13, 0
23	23, 5500, -42, 244, -174, 7, 18, 9, 32, 14, 0
24	24, 5750, -64, 249, -158, 6, 14, 6, 29, 12, 0
25	25, 6000, -85, 252, -140, 6, 14, 6, 29, 12, 0
26	26, 6250, -105, 253, -121, 6, 14, 7, 29, 12, 0

Figure 3.12: Data file example in ASCII

be stored in "78563412" format. The bits within a byte are numbered zero (least significant) to seven (most significant).

Each data sample record consists of integers arranged as follows:

**n timestamp  $A_1 A_2 \dots A_k S_1 S_2 \dots S_m$**

Where n is the sample number, timestamp is the time stamp,  $A_1 \dots A_k$  are the analog channel data values in two bytes continued until data for all analog channels are displayed and  $S_1 \dots S_m$  are the status channel data values in 2 bytes (16 bits) for each 16 or part of 16 status channels continued until data for all status channels are displayed.

Figure 3.13 shows an example binary data sample, taken from [38]. It has six analog values and six status values.

**05 00 00 00 9B 02 00 00 08 FD FA 04 48 00 3D 00 74 FF 0A FE 30 00**

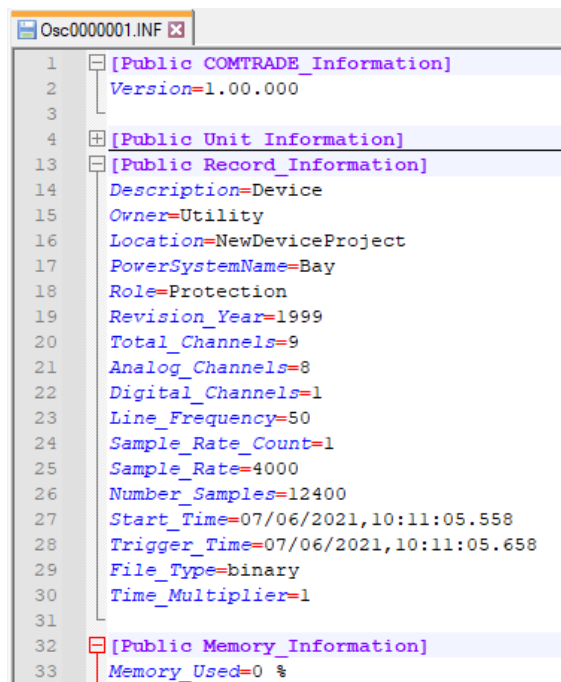
Figure 3.13: Data sample in binary format example [38]



### 3.2.1.4 Information File (.INF)

The information file is an optional file containing extra information that, in addition to the information required for minimum application of the data set, file originators may wish to make available to users. The format provides for public information that any user can read and use, and private information that may be accessible only to users of a particular class or manufacturer.

One of the information files obtained from the disturbance recording done in this work is shown in Figure 3.14.



```

1  [Public COMTRADE_Information]
2  Version=1.00.000
3
4  [Public Unit Information]
13 [Public Record_Information]
14 Description=Device
15 Owner=Utility
16 Location=NewDeviceProject
17 PowerSystemName=Bay
18 Role=Protection
19 Revision_Year=1999
20 Total_Channels=9
21 Analog_Channels=8
22 Digital_Channels=1
23 Line_Frequency=50
24 Sample_Rate_Count=1
25 Sample_Rate=4000
26 Number_Samples=12400
27 Start_Time=07/06/2021,10:11:05.558
28 Trigger_Time=07/06/2021,10:11:05.658
29 File_Type=binary
30 Time_Multiplier=1
31
32 [Public Memory_Information]
33 Memory_Used=0 %

```

Figure 3.14: Information file example

## 3.3 Summary

In this chapter, the IEC 61850 standard interaction with the substation automation systems was explained. More specifically, part 6, where the configuration of an IED in a substation is standardized, and part 7, where the communication inside a substation and all the different nodes and classes in it are addressed, were detailed.

In addition to that, the COMTRADE standard was also presented, in order to understand how the data output by an IED can be read and processed to analyse the information transmitted to it coming from the substation.



## Chapter 4

# Real-time closed-loop Testing for Electric Arc Modeling in Circuit Breakers

In this chapter, the electric arc model presented in Chapter 2 will be tested in a real-time closed-loop environment, consisting of a Real Time Digital Simulator (RTDS), a signal amplifier (Doble F6350e) and a commercial line differential protection relay (TPU D500). The objective of this closed-loop test is for the protection relay to read the circuit breaker's voltage and current and to advance COMTRADE files of the behaviour of the CB simulated in the RTDS, allowing its health indexing, detailed in Chapter 5.

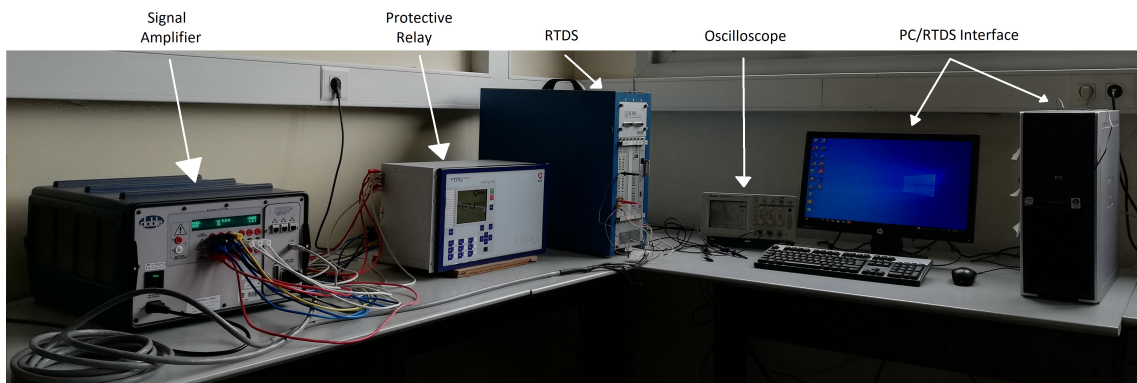


Figure 4.1: Equipment setup for closed-loop testing

### 4.1 Real Time Digital Simulator

The Real Time Digital Simulator (RTDS)<sup>1</sup> allows the simulation of real-time transient power system simulations, being a type of Electromagnetic Transients Program (EMTP). This makes it par-

<sup>1</sup><https://www.rtds.com/>

ticularly useful for the design and analysis of protection schemes, since it allows for closed-loop testing, and being a real-time simulator, the continuous voltage and current inputs allow to study the system's behaviour efficiently. However, as it is a digital simulator, it computes the power system at discrete instants of time. In this case, the time between each discrete instant, also known as time-step, is around 50-80  $\mu\text{s}$  [39].

#### 4.1.1 RTDS Software Description [40]

The high level RTDS software comprises the RSCAD family of tools. RSCAD is a software package developed to provide a fully graphical interface to the RTDS. Prior to the development of RSCAD, another software suite: PSCAD served as the graphical user interface to the RTDS hardware. RSCAD/FileManager (Fileman) represents the entry point to the RSCAD interface software. Fileman is used for project and case management and facilitates information exchange between RTDS users. All other RSCAD programs are launched from the Fileman module.

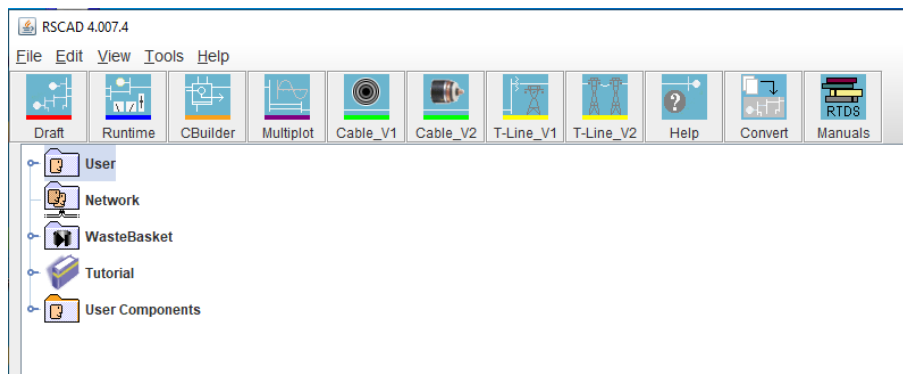


Figure 4.2: RSCAD Fileman Overview

RSCAD/Draft is used for circuit assembly and parameter entry. The Draft screen is divided into two sections: the library section and the circuit assembly section. Individual component icons are selected from the library and placed in the circuit assembly section. Interconnection of individual component icons and parameter entry follows through a series of menus.

RSCAD/RunTime is used to control the simulation case(s) being performed on the RTDS hardware. Simulation control, including start / stop commands, sequence initiation, set point adjustment, fault application, breaker operation, etc. are performed through the RunTime Operator's Console. Additionally, on line metering and data acquisition / disturbance recording functions are available in RunTime. An example of a Runtime scheme can be found in Appendix B.

RSCAD/CBuilder provides a mechanism for RTDS users to develop their own component models. Both power system and control system type components may be developed using CBuilder. CBuilder includes an interface for drawing the component's icon including its appearance in 3 Phase and single line diagram modes in RSCAD/Draft. It also provides the structure to define the parameters which must be entered by the user for the new model, as well as, a mechanism to provide input and output signals to/from the component. A compiler is included which converts the

user written C code for the model into executable code which is integrated into the RTDS software library. Upon successful compilation, the user's new model may be included within simulation cases prepared in RSCAD/Draft just as any other component from the RTDS libraries. The user's component model may be shared with other RTDS users. Only the compiled code and component icon file needs to be available for other users to include the new component into their simulation cases.

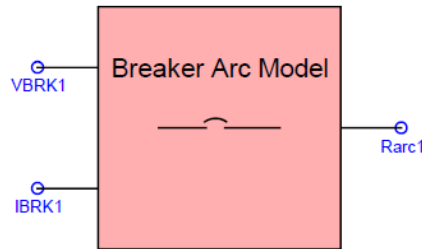


Figure 4.3: Circuit Breaker Arc Model component built in CBuilder

## 4.1.2 RTDS Hardware Description [39]

### 4.1.2.1 Giga-Processor Card (GPC)

The GPC Card is the processor card used to solve the equations representing the power system and control system components modelled within the RTDS. An RTDS rack typically contains between 2 and 6 GPC cards. The GPC card may be installed in RTDS racks which also contains 3PC cards. Each GPC card includes two IBM Power PC 750GX processors running at 1 GHz and consumes a maximum of 55 Watts. In addition to that, GPC processors may be assigned to the simulation of power electronic circuits represented using small time-step (around  $2\text{-}3\mu\text{s}$ ) components.

GPC processors include fiber ports which are used to connect various types of I/O cards (eg. GTAO (analogue output), GTAI (analogue input), GTDO (digital output), GTDI (digital input), GTFPI (front panel interface), GTNET (network interface card)).

In this work, GPC will be processing the electric arc model in the three phases.

### 4.1.2.2 Triple Processor Card (3PC)

Each Triple Processor Card contains three independent ADSP 21064 processors and their associated memory, backplane interface and input/output ports. Each 3PC contains the following I/O ports - 24 analogue output channels (12 bit,  $\pm 10$  volt range), 2 digital input ports (16 bit each) and 2 digital output ports (16 bit each). Each of the three processors (A, B and C) has access to eight analogue output channels. In addition, processors 'A' and 'B' each have access to one digital input port and one digital output port. No digital ports are associated with processor 'C'. Processor C is used for optionally available analogue I/O channels. Application of the I/O ports

varies depending upon the type of power system component model which has been assigned to run on the 3PC processors.

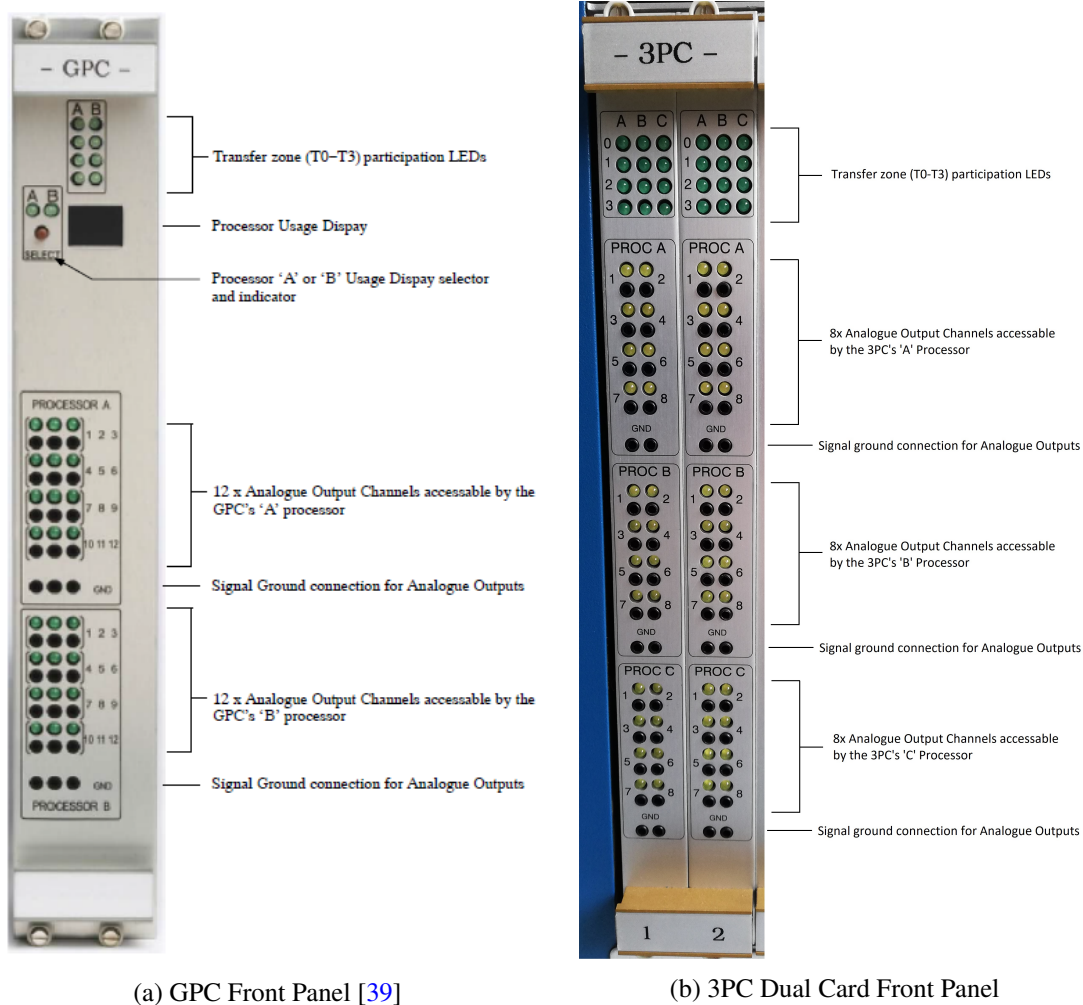


Figure 4.4: Front panel of the Processor Cards available in the RTDS rack used

#### 4.1.2.3 Workstation Interface Card (WIF)

The WIF card is usually installed on the far right side of an RTDS rack and occupies two slots in the rack. It is responsible for communication between the RTDS rack and the computer workstation running the RSCAD software, which is done over an ethernet based LAN. RSCAD/RunTime software communicates with the WIF card's real-time O/S to send and receive messages associated with plot updates and user initiated events (eg. change of a set-point via a Slider, Switch or other such RunTime component). The WIF card is also used for communication of data with the computer workstation in order to load new simulation cases, as well as, to start and stop the simulations. Communication of data between processors over the rack's backplane is coordinated by the WIF. The WIF performs self tests and runs diagnostics on other cards installed in its rack.

The diagnostics are automatically run at power up and may be initiated by the user. Results from the diagnostic tests are accessible from RSCAD [39].

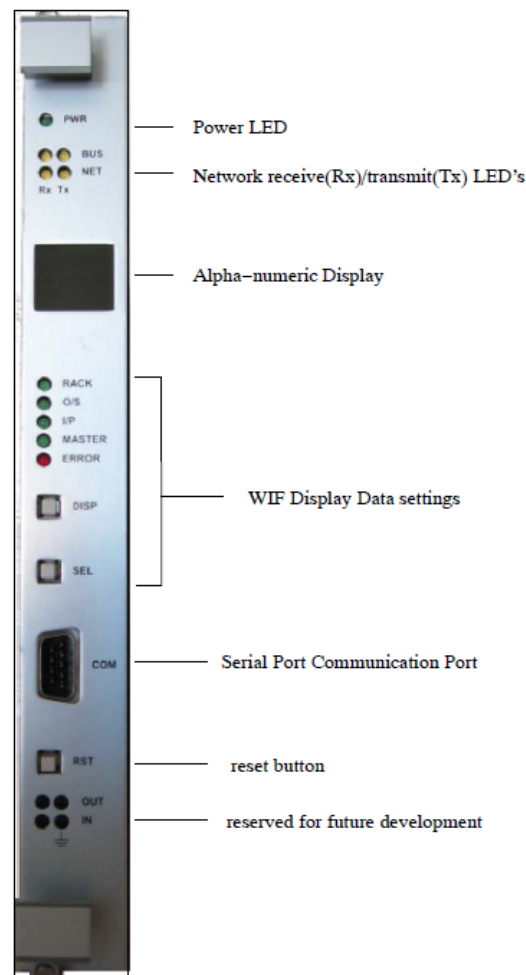


Figure 4.5: WIF Front Panel [39]

#### 4.1.2.4 Gigabit Transceiver Analogue Input Card (GTAI)

The Gigabit Transceiver Analogue Input Card (GTAI) is used to interface analogue signals from an external device to the RTDS. The GTAI card includes 12 analogue input channels with each channel configured as a differential input with an input range of  $\pm 10$  volts. Sixteen bit A/D converters are used on the GTAI card. All 12 analogue channels are sampled synchronously with new samples sent to the GPC card every  $6 \mu\text{s}$ .

#### 4.1.2.5 Gigabit Transceiver Analogue Output Card (GTAO)

The Gigabit Transceiver Analogue Output Card (GTAO) is used to interface analogue signals from the RTDS to external devices. The GTAQ card includes twelve, 16 bit analogue output channels

with an output range of  $\pm 10$  volts. The 16 bit Digital-to-Analog Converters (DACs) provide a wide dynamic range. Such a wide dynamic range may be required when using the GTAO to send measured current signals to an external protection device. The GTAO output's are oversampled at a rate of  $1 \mu s$  and the card's output channels are updated synchronously.



Figure 4.6: GTAI and GTAO 16-bit analog ports

#### 4.1.3 Circuit Breaker Electric Arc Model Simulation

The electric arc model tested before in PSCAD was implemented in RSCAD in a similar scheme and with the same parameters' values for the arc model as the one shown before. The power system's part of the scheme is shown in Figure 4.7, adapted from Appendix A.

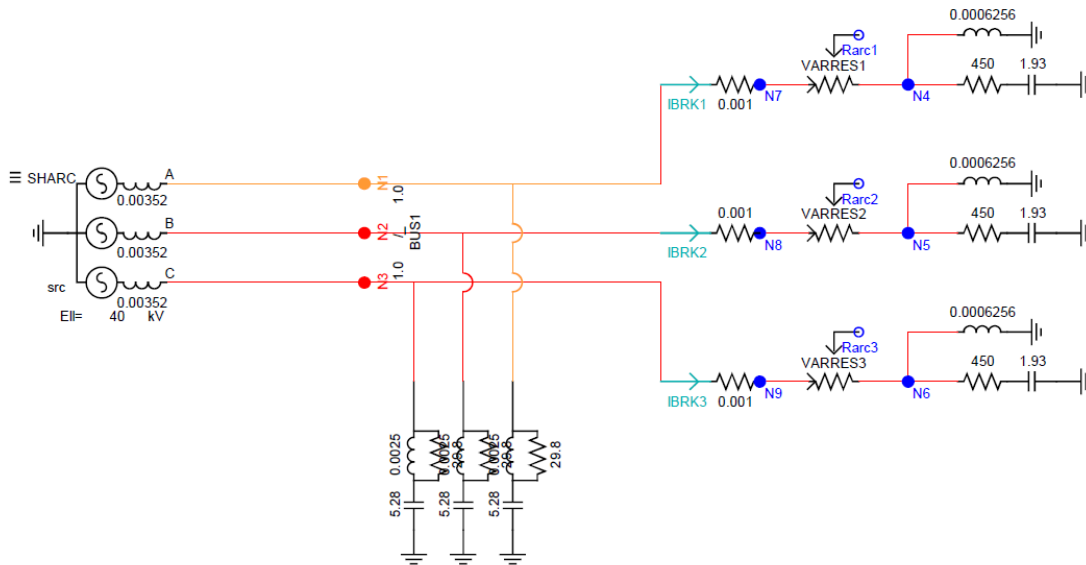


Figure 4.7: Scheme made in RSCAD/Draft to implement the Circuit Breaker electric arc model



The simulated network has 40 kV phase-to-phase and its signal frequency is 60 Hz, making it similar to the one originally made in PSCAD for easier validation of the results. In addition to that, the circuit breakers in the three phases are represented by the variable resistances VARRES1, VARRES2 and VARRES3, where their values are output by the component shown in Figure 4.3.

In this CB model, the Schavemaker equation was implemented in C code. However, in order to facilitate the coding, since implementing a differential equation would be more complex, an approach similar to the one in [41] was taken, taking the equation in 2.5 and transforming it in an incremental form:

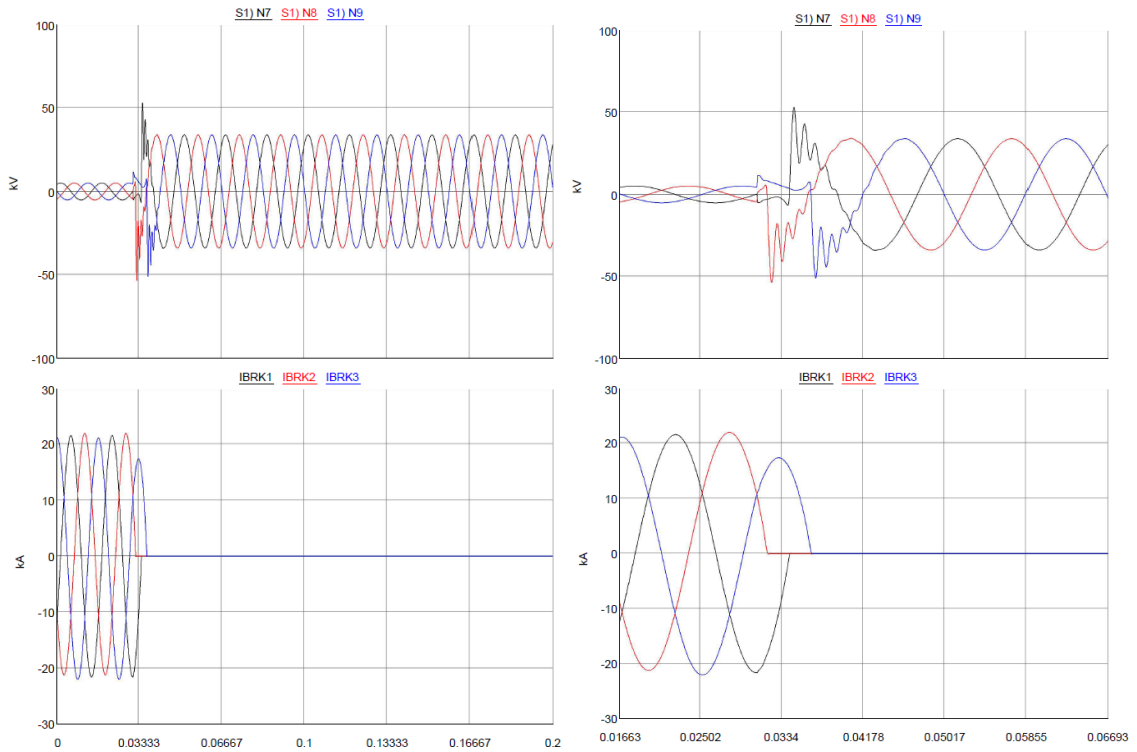
$$\frac{g_2 - g_1}{t_2 - t_1} = \frac{1}{\tau} \left( \frac{i^2}{\max(U_{arc}|i|, P_0 + P_1.u.i)} - g_1 \right) \quad (4.1)$$

Simplifying this equation, and assuming  $\Delta t$  as a small time-step resulting from  $t_2 - t_1$  we get the following result:

$$g_2 = \frac{\Delta t}{\tau} * \frac{i^2}{\max(U_{arc}|i|, P_0 + P_1.u.i)} + g_1 \left( 1 - \frac{\Delta t}{\tau} \right) \quad (4.2)$$

Making it an incremental equation, easily implemented by saving the last iteration's output value and using it in the next cycle as  $g_1$ , while  $\Delta t$  is the RTDS time-step.

To validate the implementation, the voltage and current in the simulated CBs were measured using the RSCAD/Runtime to plot their values. The results are shown in Figure 4.8:



(a) Voltage and Current plots

(b) Plots zoomed in the CB opening timestamp

Figure 4.8: Voltage and Current measurements in all three phases in RSCAD/Runtime

In addition to that, in order to check if the D/A outputs were correctly outputting the desired values and double-check the implementation validation, one phase voltage and current was output to the D/A outputs present in the 3PC front panel and measured with the oscilloscope available at the Laboratory, obtaining the measurements visible in Figure 4.9.

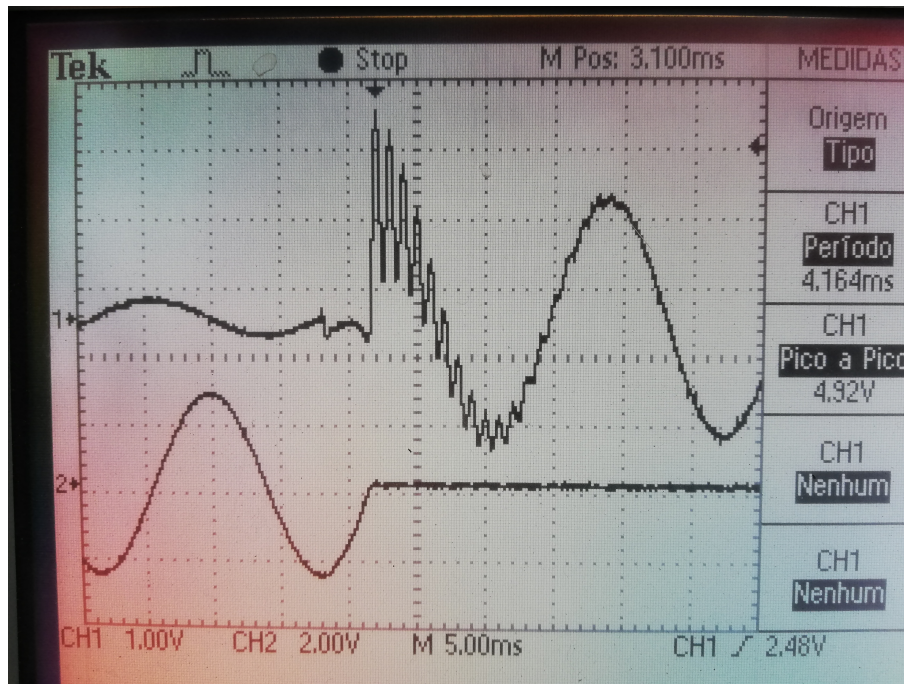


Figure 4.9: Single Phase Voltage and Current measurements in the Circuit Breaker

After these two validations, it can be concluded that the arc model was correctly implemented and the three phased signals can be correctly output to the digital relay for analysis and studying of the waveforms. The outputs used will be the 3PC front panel 12-bit resolution analog ports, which even though they are not usually recommended for external equipment connection, gave good results, confirmed by the oscilloscope measurements, and the RTDS 16-bit analogue output signals were having noise interference which impact on the overall signal was too considerable to be used.

## 4.2 Doble F6350e Signal Amplifier

For the voltage signals to be correctly read and interpreted by the IED, they need to be in a bigger scale, since the analog outputs from the RTDS have a maximum range of -10/10 Volts. Moreover, the current signals are output as voltages by the RTDS, and they need to be converted to their corresponding current values. For this effect, the Doble F6350e amplifier was used.



Figure 4.10: Doble F6350e Signal Amplifier

The signal amplifier is capable of outputting voltages of up to 75/150/300 V and currents of up to 8.75/17.5/35 A in the normal 3V & 3I setup [42]. However, as there was no need for the current values to be so high to be correctly read by the IED, the 3V & 3 Low I configuration was chosen, with  $V_A$ ,  $V_B$  and  $V_C$  having a maximum range of 75 Volts and  $I_R$ ,  $I_S$  and  $I_T$  going up to 1 A, as shown in Figure 4.11.

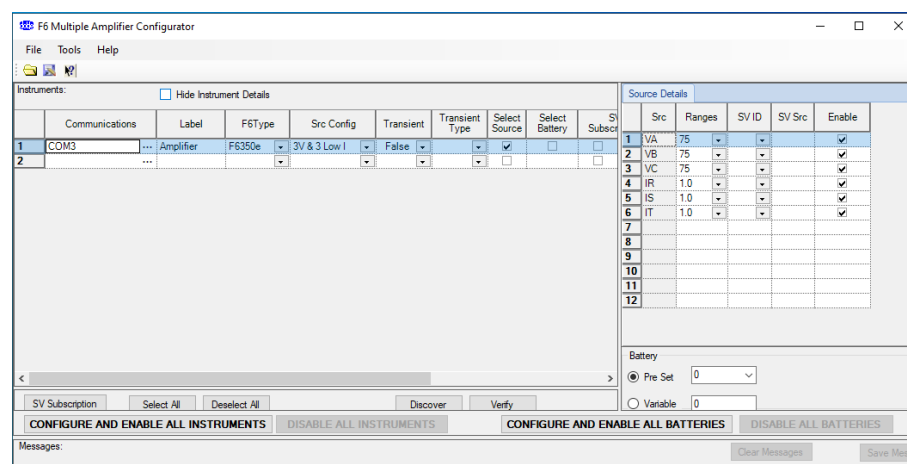


Figure 4.11: Configuration of the F6350e Amplifier

The connection between the RTDS and the F6350e was done through the 05B-0730-05 Universal Low-Level Cable provided with the amplifier, connected to the 3PC D/A 12-bit outputs. Figure 4.12 shows the detailed description of the Low-Level Cable used, taken from [42]:

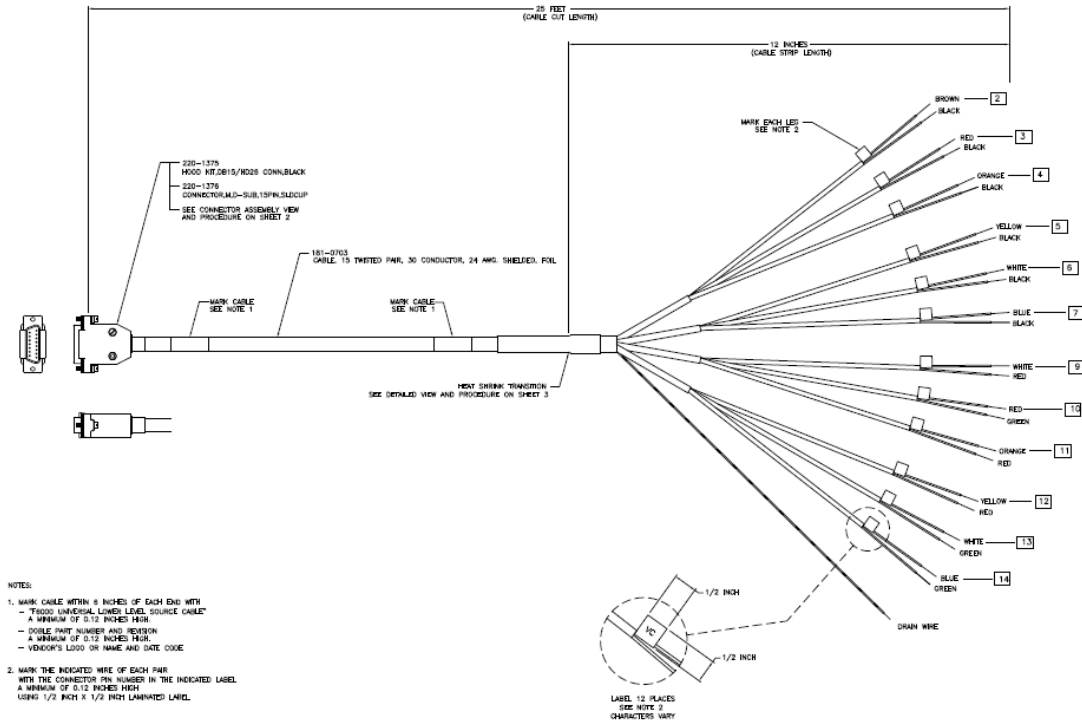


Figure 4.12: Cable used to inject Low-Level Signals into the Signal Amplifier [42]

### 4.3 Finalizing the closed-loop test by recording the simulated disturbances



Figure 4.13: TPU D500

The final part of the closed-loop setup is the digital relay available at the Laboratory, the Efacec TPU D500. This IED was connected to the amplified signals from the F6530e, as seen in Figure 4.14, in order to measure all three phases voltage and current signals in the simulated circuit breakers and record them if a fault occurred.

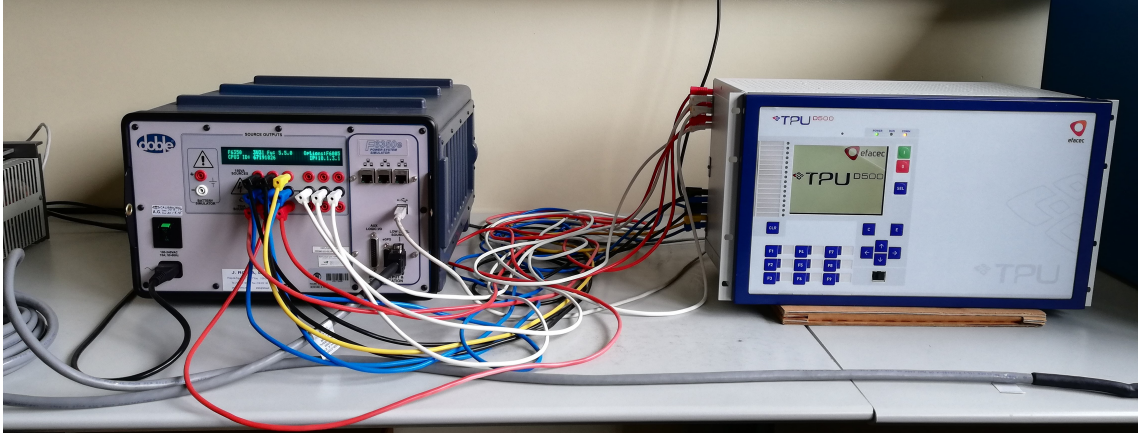


Figure 4.14: Connection between the F6530e and the TPU D500

With the signals being correctly captured, the IED was configured, through Efacec's Automation Studio software, to record and save the waveforms of the inputs whenever the voltage values read reached more than 30 kV. This value was concluded through observing that, before the CB opening, the peak voltage did not reach values higher than 10 kV, while the peak of the TRV would normally reach values of around 50 kV. Therefore, any peak voltage superior to 30 kV would be the result of the CB tripping, being interpreted as a disturbance and recorded by the TPU D500.

One of these recordings is shown in Figures 4.15 and 4.16, where it is possible to verify the preservation of the signal from the RTDS to the IED.

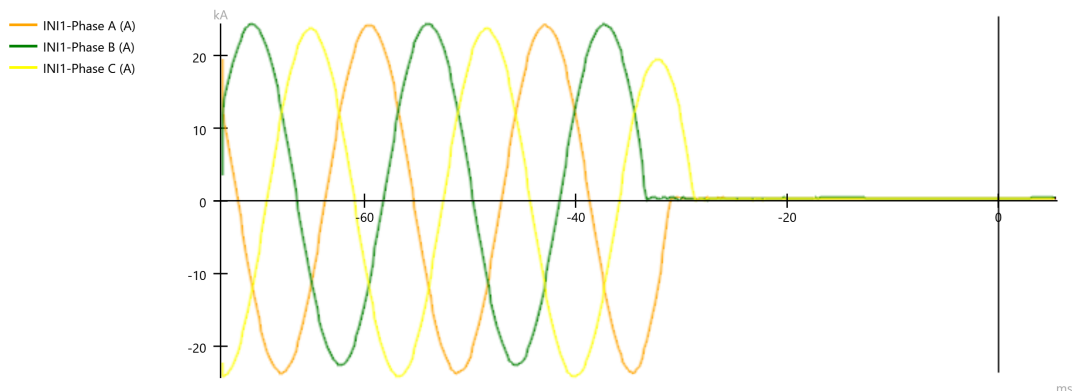


Figure 4.15: 3-Phase Current measured during the recorded disturbance

In total, eighteen different simulations were made (simulating 54 different single-phased circuit breakers), some of them having some alterations. One of this changes was on the parallel's



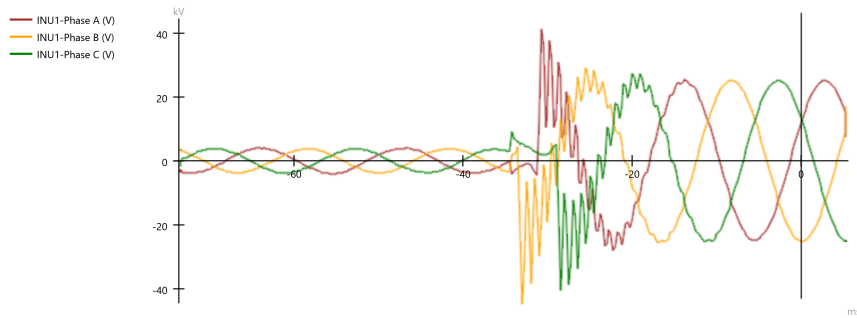


Figure 4.16: 3-Phase Voltage measured during the recorded disturbance

RLC circuit values, in which decreasing the L's value increased the time duration of the transient recovery period. The other approach taken was to change the electric arc model's parameters,  $\tau$ ,  $P_0$ ,  $P_1$  and  $U_{arc}$  from their original functioning values (detailed in Section 2.4.3.4). Both these factors produced waveforms which could represent worn or malfunctioning circuit breakers, being able to give a bigger data sample for analysis and final standardization of the health indexing.

The closed-loop full scheme used for this work is detailed in Figure 4.17:

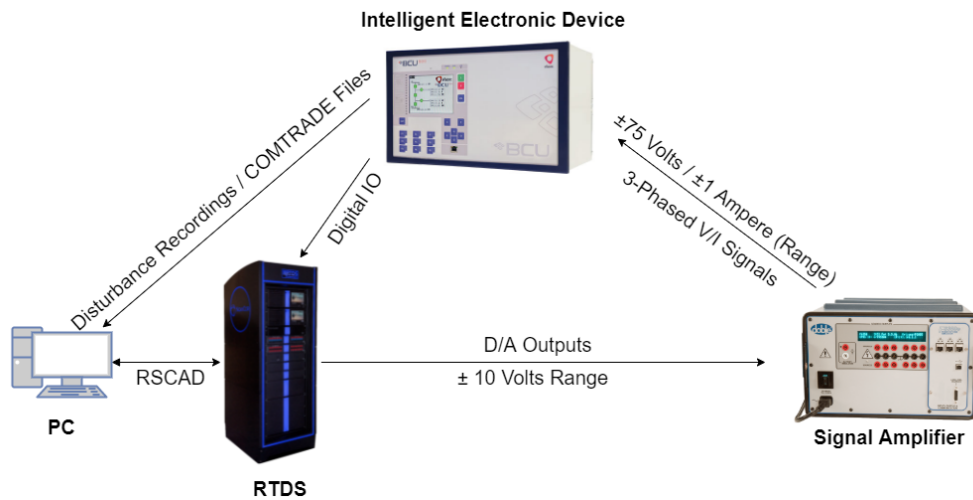


Figure 4.17: Interaction between all the equipment in the closed-loop test

## 4.4 Summary

This chapter presented a closed-loop simulation of the behaviour of a circuit breaker during an opening operation, the final output being an IED for further signal analysis. In addition to that, the equipment and software necessary for this test were explained, detailing each one's role in the closed-loop scheme.

Finally, the results obtained were shown, validating the process taken during this phase.

## Chapter 5

# Creating the Health Index for the Circuit Breaker

Finally, in this chapter, the waveforms recorded in Chapter 4 were analysed in order to create a health index algorithm for the circuit breakers, with two distinct phases, the online indexing and offline indexing.

For this effect, through Efacec's Automation Studio, all the simulations were exported as COMTRADE files. With these set of COMTRADE files, each recording configuration and data files were read. The configuration file is read to identify the existent channels, their range, the time in which the disturbance occurred and in which format the data file was exported (ASCII or binary) and after this information is decoded, it is possible to read the data file and decode it into numeric variables (as detailed in section 3.2.1.3).

This decoding was done into the MATLAB<sup>®</sup> software, in which each channel's numeric values from every simulation were recorded as a numeric vector, making it in total 54 different variables for analysis, each one representing one CB. In order to validate the decoding, the signals were shown using MATLAB's plotting capabilities, resulting in waveforms similar to Figures 5.1 and 5.2, being in concordance with the results obtained in the previous chapters.

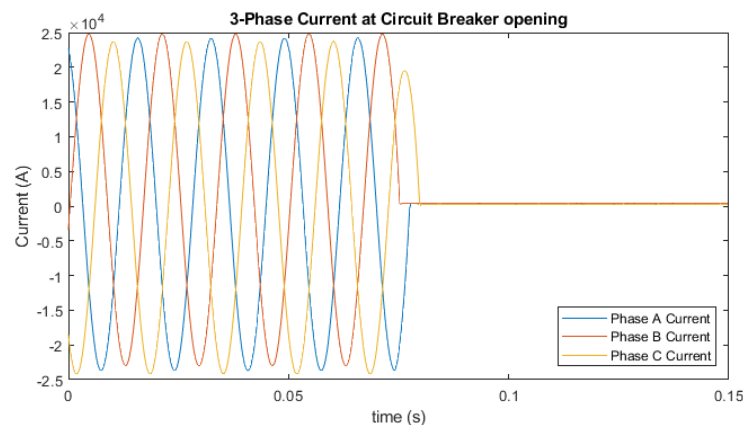


Figure 5.1: Waveforms of all three phases' current during a recorded disturbance

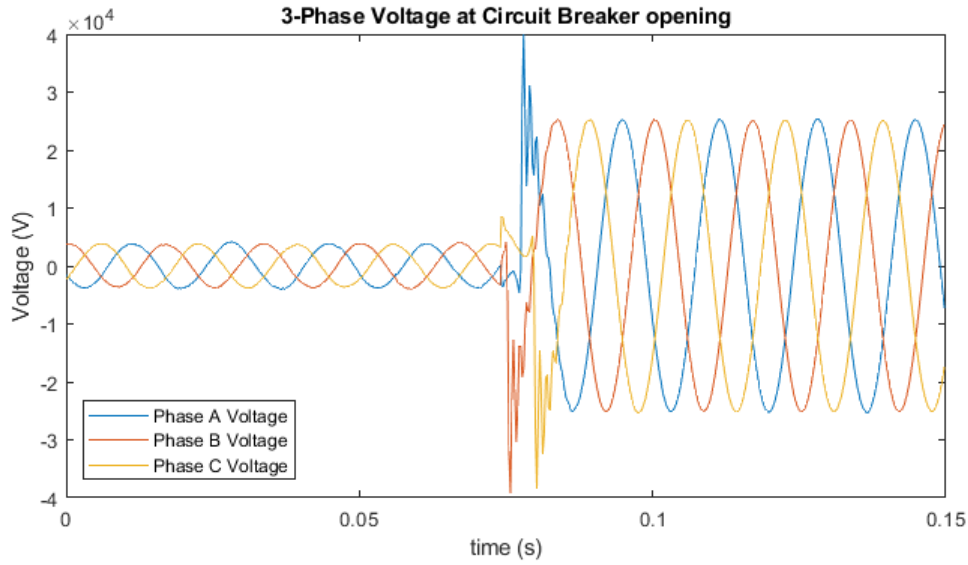


Figure 5.2: Waveforms of all three phases' voltage during a recorded disturbance

## 5.1 Online Parameters Analysis

The first analysis in this work is meant to be done while the circuit breaker is still working normally, without the need of disconnecting it from the grid. This can also be referred as an online analysis of the CB.

However, in this situation, specific tests are not possible, and the analysis is restricted to information provided by sensors and current/voltage transformers. In this work, only the COMTRADE files data will be used. Therefore, only the information that would normally come from the current and voltage transformers will be considered.

The three parameters considered for this phase were:

1. Opening time, measuring the time since the CB started opening to the moment of arc extinction;
2. Current RMS value after opening, measuring the RMS value of the current from the moment the arc extinguished;
3. Duration of the transient recovery period, measuring the time the voltage waveform oscillated at a high frequency after the current crosses the zero value.

### 5.1.1 Circuit Breaker Opening Time

This parameter is based on the time between the beginning of the opening of the CB to the moment the arc is extinguished completely and the current has a stable value, normally null. Figure 5.3 shows in detail how the measurement was done, the procedure being the same for every record analysed.



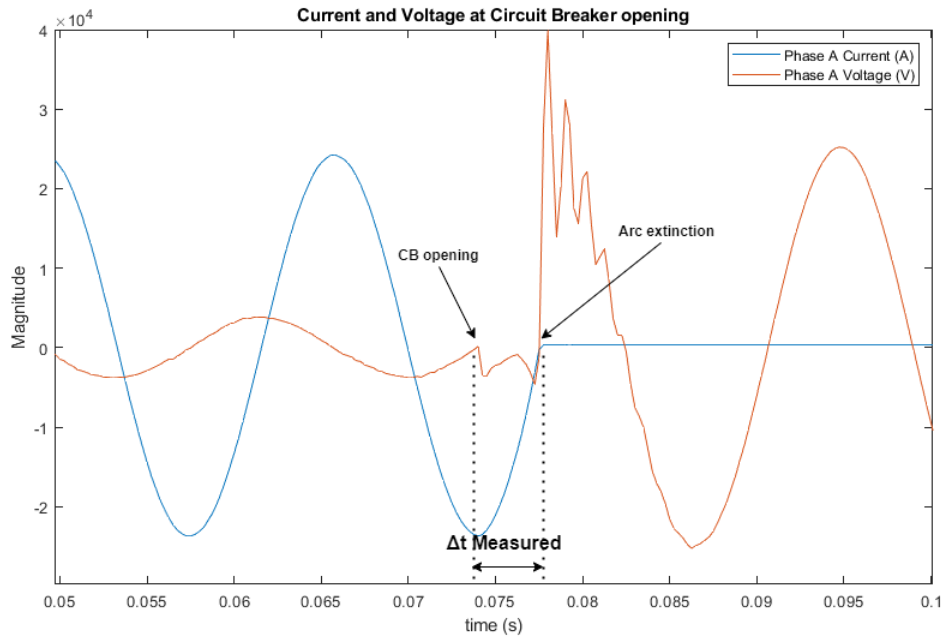


Figure 5.3: Opening Time measurement procedure

For it to have any considerable value, a sample of recordings with standard values for all circuit and arc model parameters were read, and a gaussian distribution function was applied to the measured opening times. This produced the graph visible in 5.4:

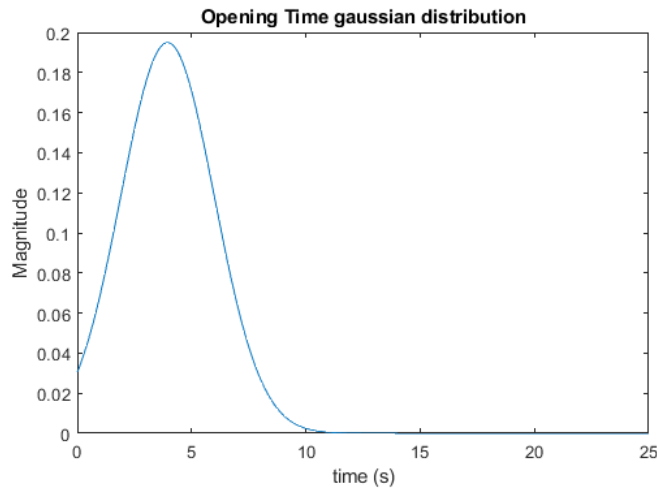


Figure 5.4: Opening Time normal distribution applied to the sampled data

The curve obtained, with a maximum value of 0.1949, a mean value ( $\mu$ ) of 3.94691 seconds and a standard deviation ( $\sigma$ ) of 2.04641 seconds, was converted into a 0 (very poor) to 1 (excellent) classification scale, in order to standardize all the different parameters' results. Then, it was applied to the measured opening times. A histogram of all the results obtained was created and is visible in Figure 5.5.

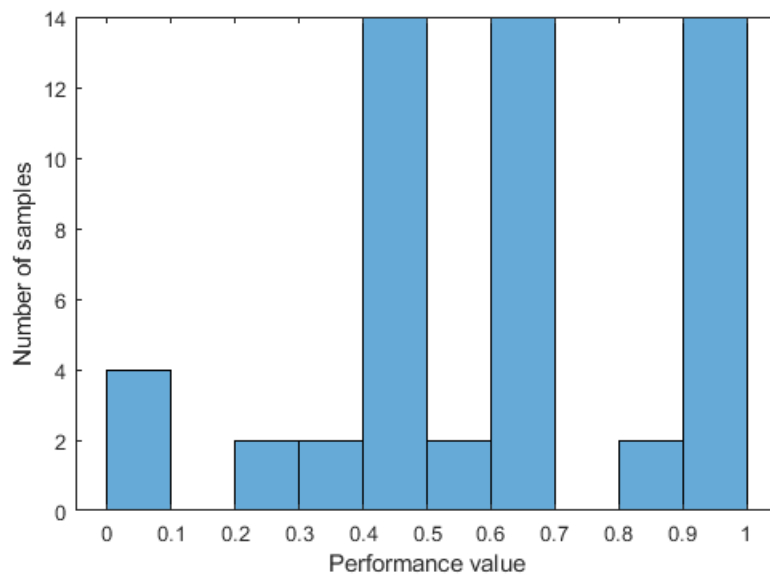


Figure 5.5: Distribution of all records' Opening Time performance

From this histogram, it can be concluded that most recordings stand at an acceptable value, but there is still a considerable sample reaching poor performance levels ( $\leq 0.5$ ). This is justified by the fact that since these are recordings taken from simulations, the distribution function created has a small standard deviation value, being sensitive to deviations of more than 2 seconds which are not that unlikely to occur. Below are two examples of recordings, one which reached a very high performance level and one who had poor results on it.

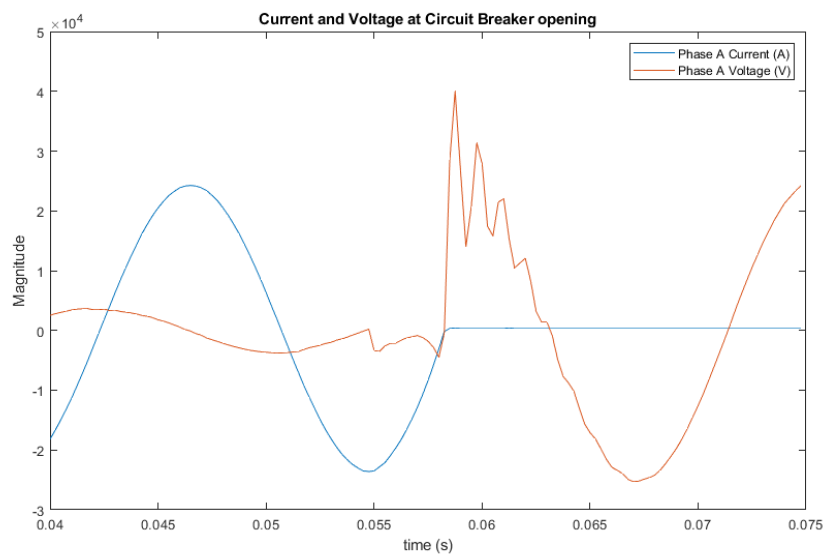


Figure 5.6: Voltage and Current plots of an opening with good performance results

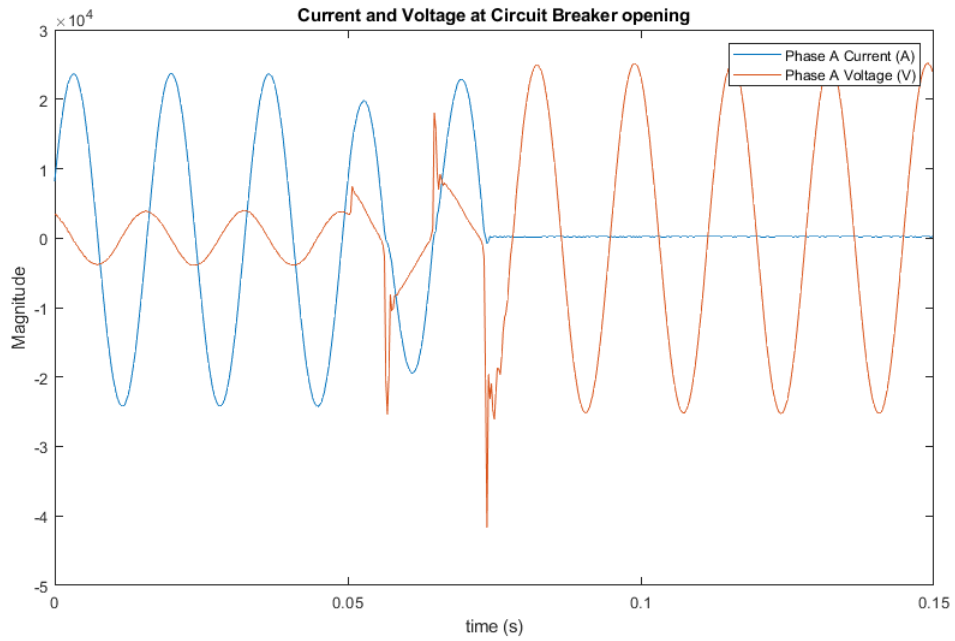


Figure 5.7: Voltage and Current plots of an opening with poor performance results

Observing the two examples, it can be concluded that while Figure 5.6 had good results as the opening time, in this case 3.755 seconds, was close to the mean value, Figure 5.7 suffered arc re-ignition and only managed to extinct it after 2 cycles, having a total opening time of 24.006 seconds, differing too much from the distribution's mean value and therefore having a performance result close to 0.

#### 5.1.1.1 Opening Time Results Interpretation

With all these results, this factor can be validated as a method of concluding if the circuit breaker's contacts are not worn or damaged, verifying if their opening time is close or not to the expected value taken from the available data sample. In addition to that, it can be a method of verifying if the CB is properly extinguishing the arc, as re-ignitions will result in a bigger measured opening time.

### 5.1.2 Current Root Mean Square Value after Circuit Breaker opening

The second factor analysed is the current RMS value after the arc extinguished, meaning the opening process was concluded. Figure 5.8 exemplifies where and how the measurement is done for each waveform recorded.

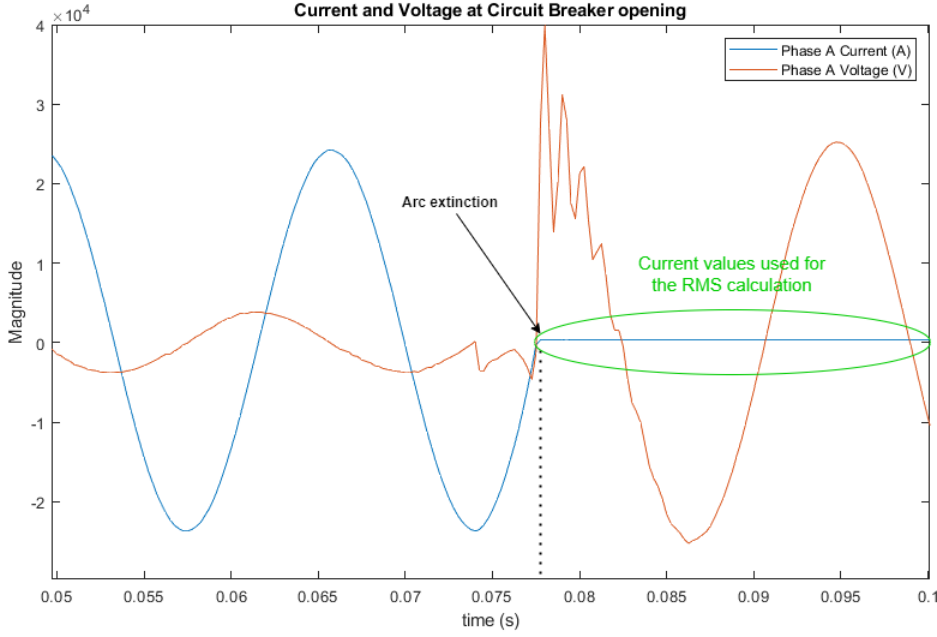


Figure 5.8: Current RMS value measurement procedure

This RMS value is calculated using the following formula:

$$I_{RMS} = \sqrt{\frac{1}{T_2 - T_1} \int_{T_1}^{T_2} [i(t)]^2 dt} \quad (5.1)$$

Where  $T_1$  and  $T_2$  are the moment arc is extinguished and the end of the recording sample, respectively.

After the current values were measured for all recordings, a similar approach to the previous section was taken, with the creation of a normal distribution function for the classification of the RMS values. In this case, the parameters for the distribution function are:  $\mu = 0$  A and  $\sigma = 5$  A. The gaussian distribution obtained is shown in Figure 5.9.

The scale from the distribution function was then converted to a 0 to 1 scale, exactly as in the opening time parameter, and applied to the recordings, producing the histogram visible in Figure 5.10.

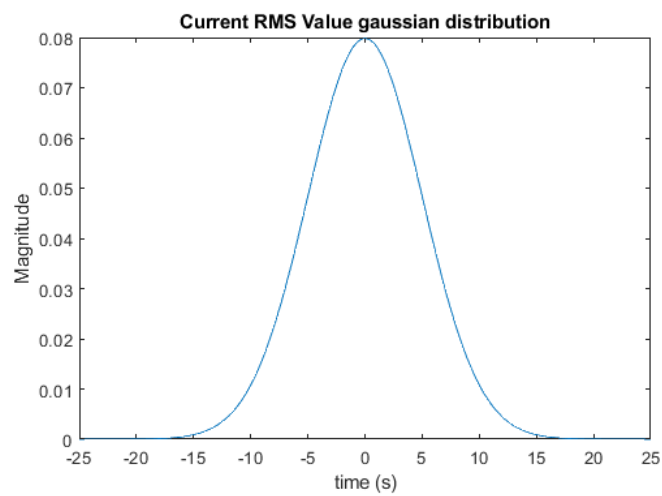


Figure 5.9: Current RMS Value normal distribution applied to the sampled data

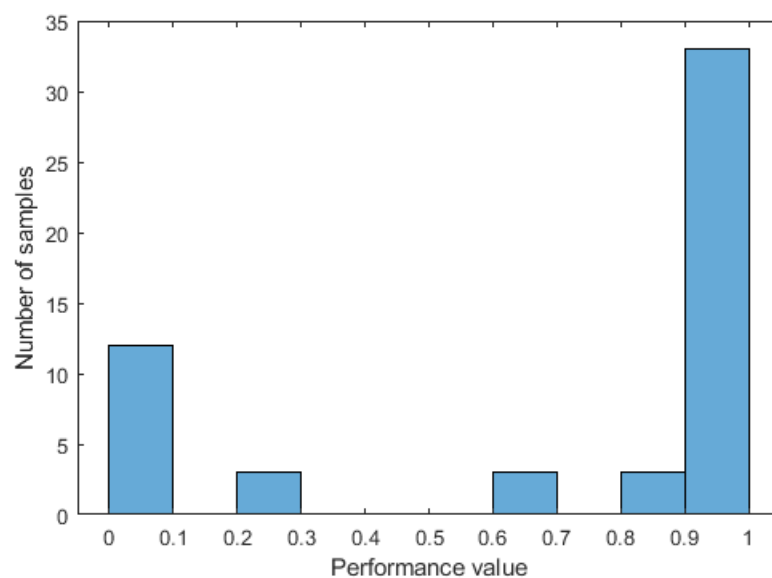
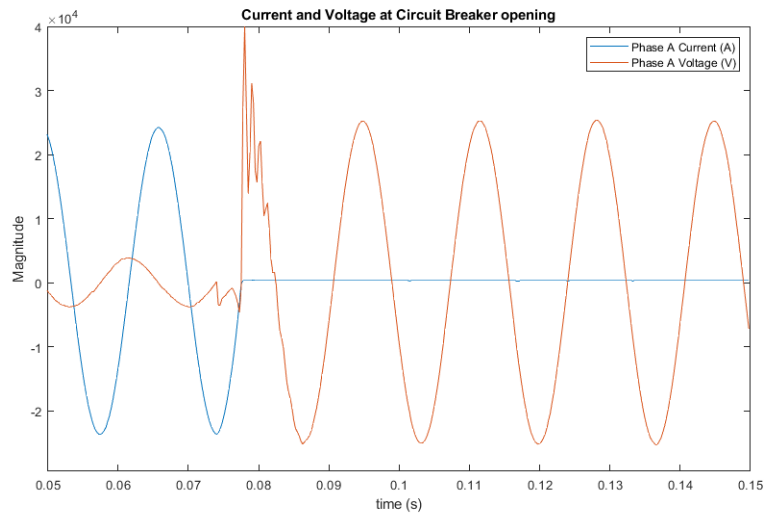
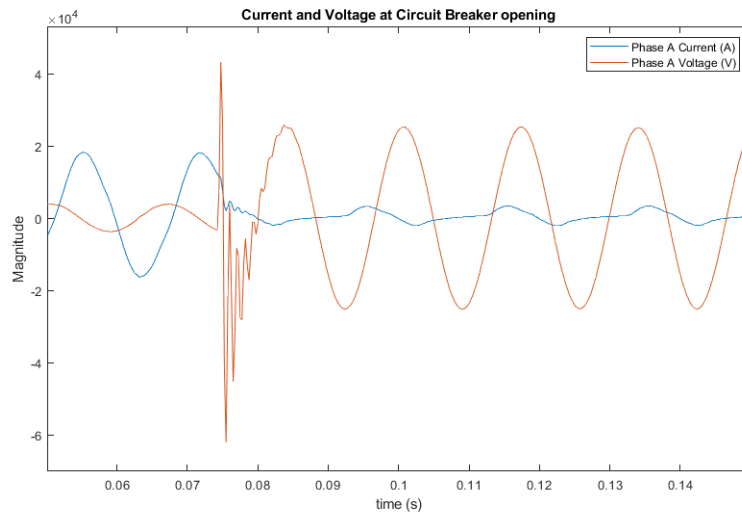


Figure 5.10: Distribution of all records' Current RMS Value performance

As expected, most of the recordings had a very good evaluation in this parameter, with more than 50% of the samples having a performance value between 0.9 and 1, with the current staying null after the zero-cross period. The poor results from the simulation can be due to noise in the RTDS outputs, which result in variations of around 200 A in the IED measurements, or in simulations where some parameters were changed and the current flow was not completely stopped after the opening of the CB.



(a) RMS measurement with good performance results



(b) RMS measurement with poor performance results

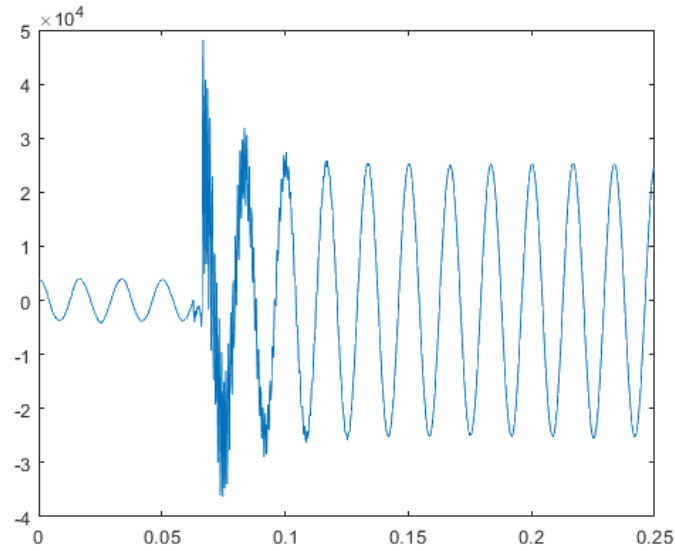
Figure 5.11: Voltage and Current plots of two distinct RMS measurement recordings

### 5.1.2.1 Current RMS Value Results Interpretation

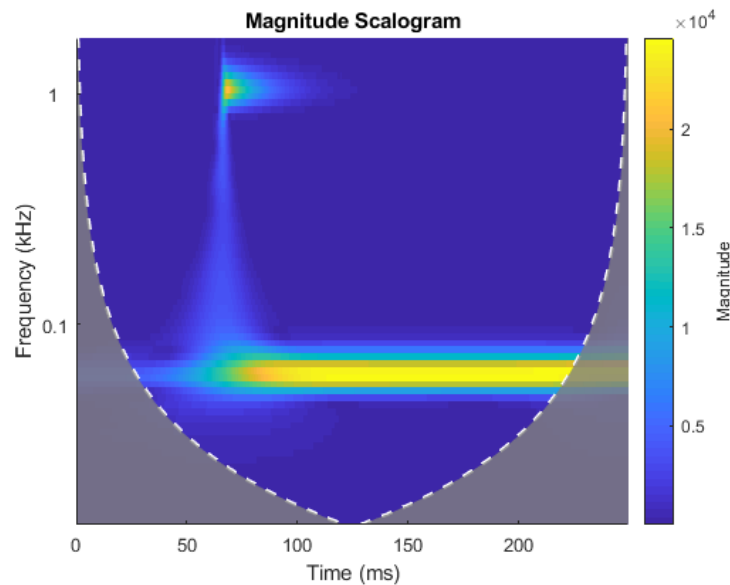
Considering these results, this parameter can be seen as an effective way to verify if the CB is functioning correctly in its opening process and not letting any residual current go through, whether it is because the contacts did not open correctly and/or there is a defect in the CB resulting in it malfunctioning.

### 5.1.3 Transient Recovery Voltage duration

The final factor analysed was the duration of the TRV after the zero-current cross. This was done through a time-frequency analysis of the captured signal, by using the continuous wavelet transform, available in the MATLAB® software.



(a) Single-phase Voltage of a recorded disturbance



(b) Continuous Wavelet transform of the signal

Figure 5.12: Comparison between the voltage waveform of a signal and its wavelet transform

As seen in Figure 5.12, the duration of the TRV is difficult to calculate through voltage measurements. However, since the wavelet transform separates the different frequencies existent in the signal, it is easy to separate the transient component from the steady-state component during

the TRV, and measure the transient component's duration.

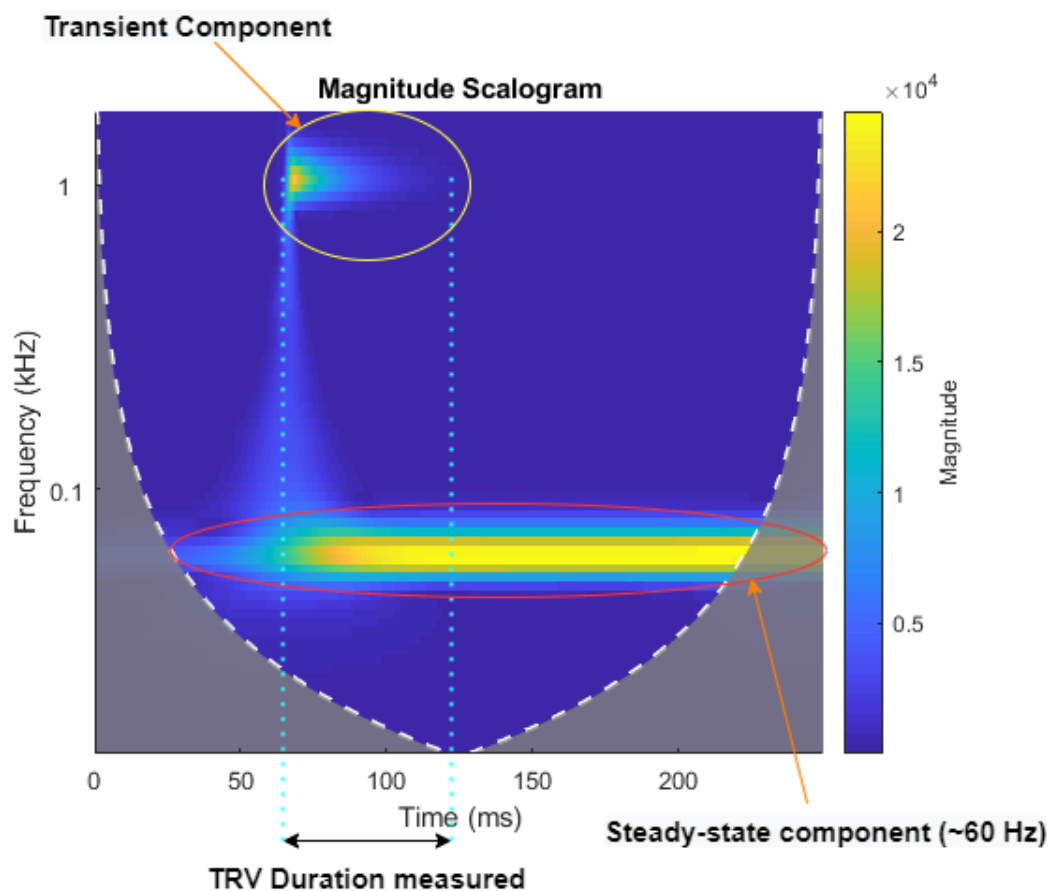


Figure 5.13: TRV duration measurement procedure

After measuring all recordings, the samples which had the standard parameter values were used to create a gaussian distribution, which resulted in a curve with  $\mu = 9.10417$  seconds and  $\sigma = 2.09853$  seconds, as seen in Figure 5.14.

This distribution was applied to all recordings and their performance values were converted into the 0 to 1 scale used before, producing the histogram visible in Figure 5.15.

From the results obtained, it can be concluded that most recordings had a good performance in the TRV duration parameter, while the group of poor results originate from alterations in the circuit (for example, less inductance in the parallel RLC circuit) or circuit breakers which had problems after the zero-cross and took longer to stabilize.



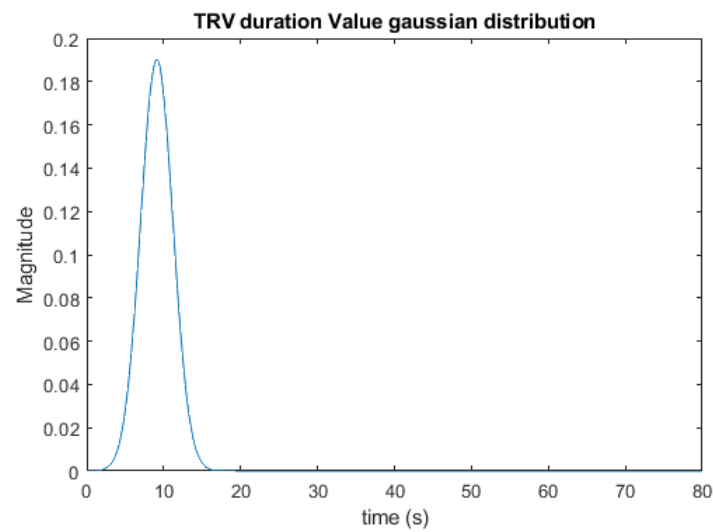


Figure 5.14: TRV duration Value normal distribution applied to the sampled data

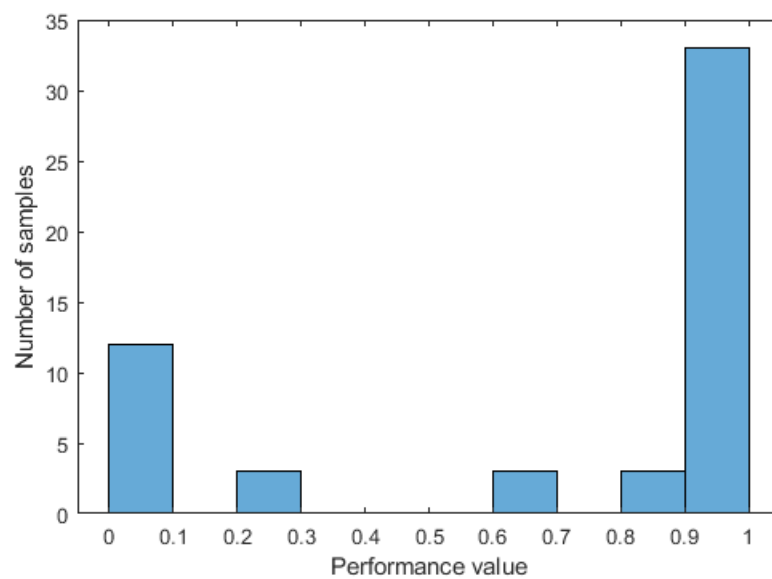


Figure 5.15: Distribution of all records' TRV duration performance

#### 5.1.4 Weighting the Online Parameters

The remaining part of the online indexing process is to sum all the performances together. For that to happen, however, each one needs to be given a weight for the final calculation.

The opening time and current value after opening are important factors to check if the CB is malfunctioning, and therefore they were given the same weight of 40% each. As for the TRV duration, it is not a direct indicator of the CB not being able to work properly anymore, only giving signals of it being worn or the circuit around it having some flaws, and was given a weight of 20%.

The formula can then be represented by:

$$TOTAL_{value} = 0.4 \times Open_{value} + 0.4 \times RMS_{value} + 0.2 \times TRV_{value} \quad (5.2)$$

Applying this formula to every sample, the final indexing obtained is shown in Figure 5.16.

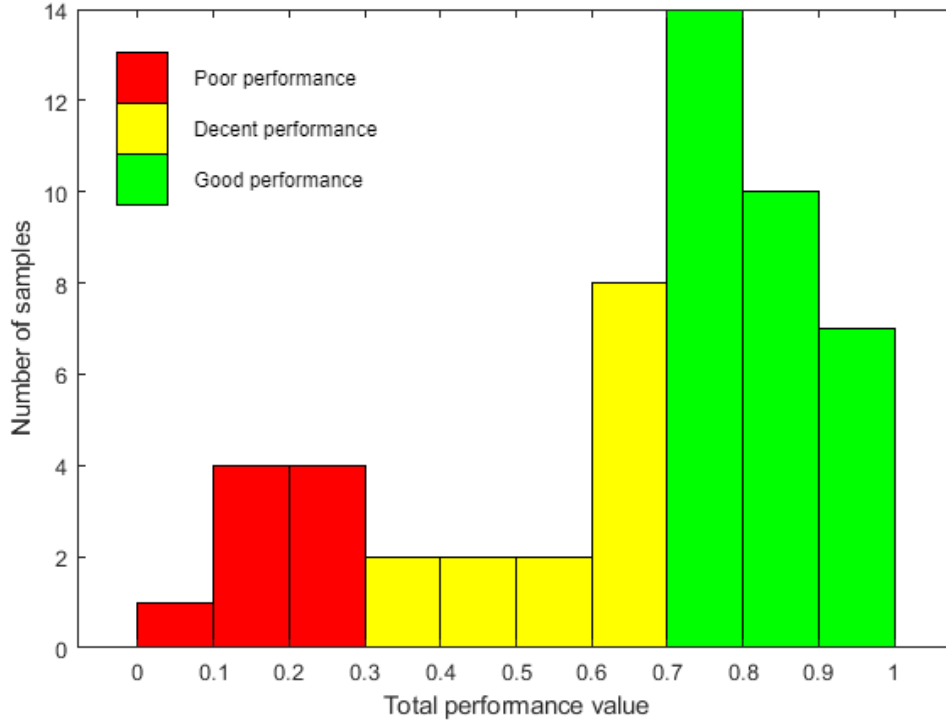


Figure 5.16: Total performance of all recordings

After obtaining the online health index of the circuit breaker, the following procedure is suggested according to its performance value:

- Good performance (0.7-1) - No additional tests required, as the CB is in good shape;
- Decent performance (0.3-0.7) - The CB may be worn, but is still able to function properly. Additional tests (mentioned further in this Chapter) should be done in the next scheduled maintenance;
- Poor performance (0-0.3) - The CB is damaged/malfunctioning. It should immediately be removed from the grid and additional tests should be done to verify what the problem is.

## 5.2 Offline Parameters Analysis

Although the online parameters are good indicators of whether the circuit breaker is in good condition or malfunctioning, it does not give a precise indication of where or what the problem is. To complement that, when the CB does not perform well in the online tests, additional specific tests are suggested. These are grouped into three categories, them being:

1. Dynamic contact Resistance Measurement;
2. Time-travel analysis;
3. Minimum pick-up voltage.

### 5.2.1 Dynamic contact Resistance Measurement

The first offline parameter analysed is the Dynamic contact Resistance Measurement (DRM). This analysis is primarily done on SF<sub>6</sub> breakers, to determine if their arcing contacts are in good condition or worn/damaged. For this effect, a high DC current of at least 100 A is applied to the CB's terminals, while measuring the voltage drop across the breaker's contacts, the injected current and the breaker contact travel curve during an opening operation. This opening operation should be done at a low contact speed (between 0.002 - 0.2 m/s), as doing it at rated speed does not give any meaningful results [43]. This comparison is shown in Figure 5.17.

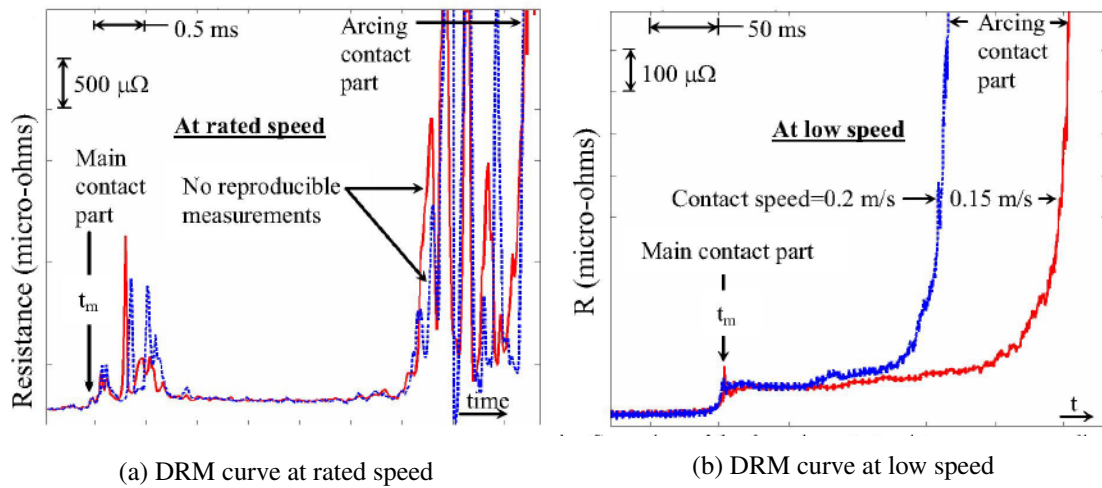


Figure 5.17: Comparison between rated and low speed in the dynamic resistance measurement (taken from [43])

The DRM curve is acquired by dividing instantaneous voltage to current. After obtaining it, its features must be analysed in order to determine the contacts condition. The main features considered are [44]:

- $R_a$ , the average arcing contact resistance before the vertical slope of the DRM curve;
- $R_p$ , the average main contact resistance;

- $R_a \cdot T_a$ , the cumulative area beneath the DRM curve just before the maximum value reached (before the arcing contact part);
- $T_{ov}$ , the time difference between separation of the main and arcing contact;
- $R_{a,max}$ , the maximum value of resistance before the arcing contact part.

These diagnosis features are shown in Figure 5.18:

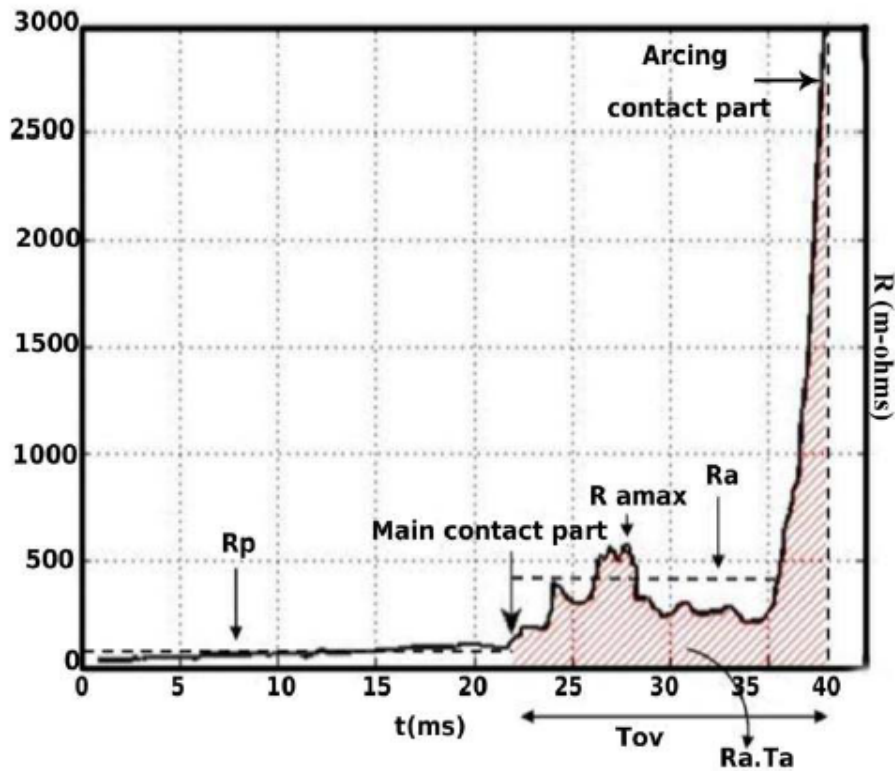


Figure 5.18: DRM curve with the diagnosis features [44]

These parameters are given performance scores based on their comparison to the distribution curve, similar to the one done in the online analysis, and to sum their parts together they are given weights, resulting in the final health index (HI) formula:

$$HI = \sum_{i=1}^5 (p_i * w_i) \quad (5.3)$$

Where  $p_i$  is each feature's performance score, and  $w_i$  is the relative weight given to it.

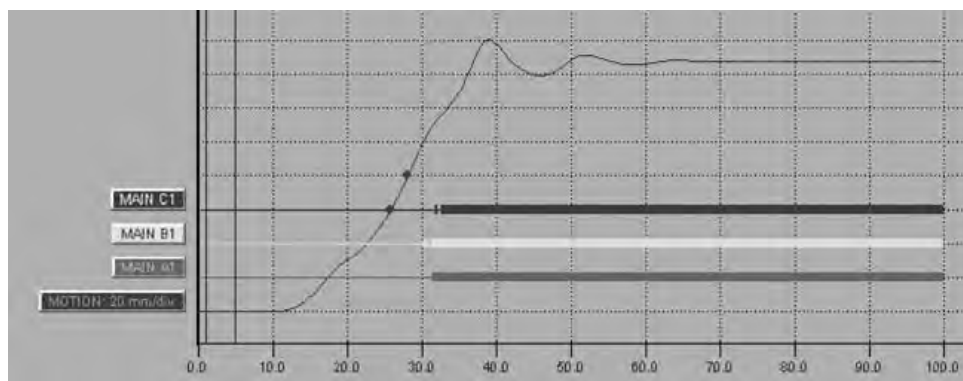
After calculating the health index, it is possible to determine if the CB's arcing contacts are in good condition or if there is a need for preventive/corrective maintenance, such as suggested in [44].

### 5.2.2 Time-travel analysis

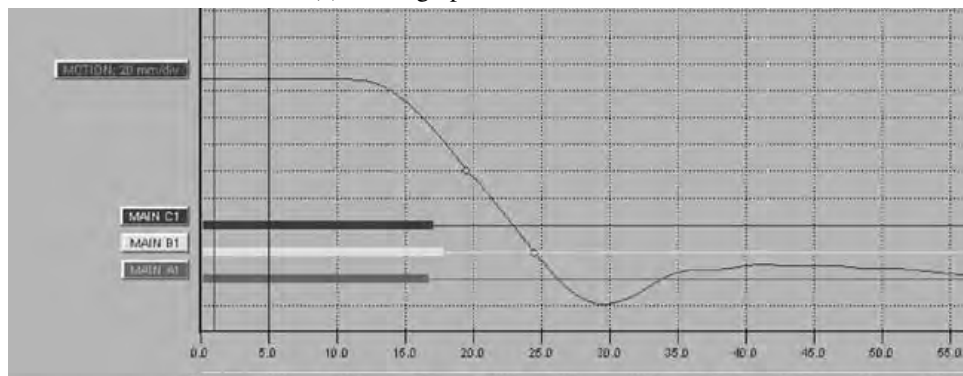
The next test assesses the electrical and mechanical condition of the CB, and is usually done to detect problems in the breaker operating mechanism [45]. It can be split in two distinct sets of analysis: Operating timings and capabilities and Contact positioning measurement. All the parameters are compared to typical values to verify if the CB needs maintenance or is behaving as intended.

#### 5.2.2.1 Operating timings and speed

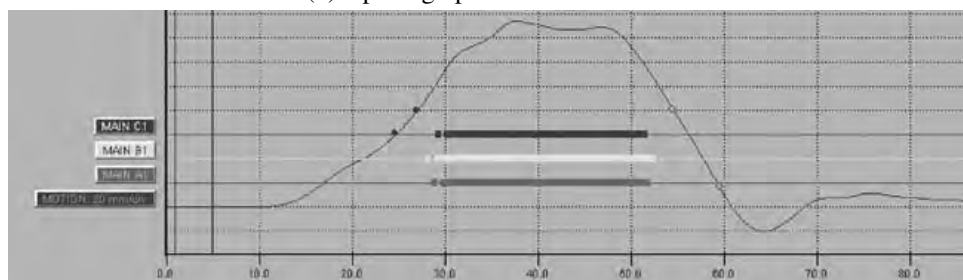
The first set of tests monitorizes the tripping and closing operations, trip-free operation (simulates the condition when an open breaker is closed into a fault and then it is tripped free by a protective relay) and trip-reclose operation.



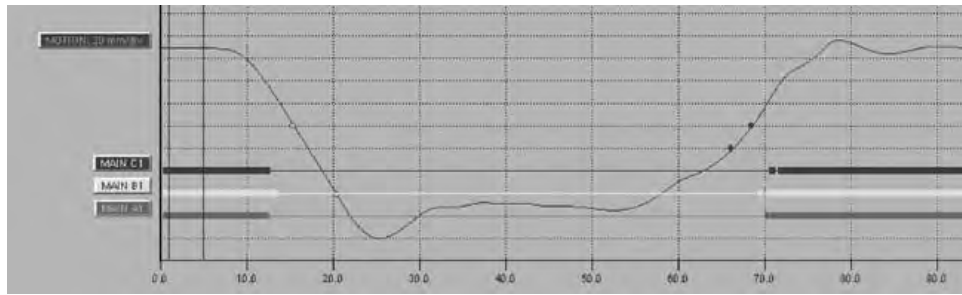
(a) Closing operation of a breaker



(b) Opening operation of a breaker



(c) Trip-free operation of a breaker



(d) Trip-reclose operation of a breaker

Figure 5.19: Circuit Breaker operating tests (taken from [45])

In the opening and closing tests, the operating time is measured to assure that it is inside acceptable limits. In addition to that, the operating speed is also considered, as a slow operation due to ageing or degradation can compromise the protection and coordination scheme of the protective relays. The trip-free operation confirms whether a breaker, if closed into a fault, can clear it, while the trip-reclose operation assures that the breaker closing time is within specified limits after a trip operation [45].

### 5.2.2.2 Contact positioning measurement

The second set of tests goes over the positioning of the breaker's contacts during a closing operation. In it, the following characteristics are analysed [46]: **Total Travel**, the distance traveled by the contacts between the initial starting position to the final resting position; **Over Travel**, the distance traveled by the contacts exceeding the final resting position; **Rebound**, the distance traveled by the contacts beyond the final resting position after returning from over travel; **Stroke**, the maximum distance traveled by the contacts during the closing operation. Figure 5.20 exemplifies one closing operation with all these characteristics detailed.

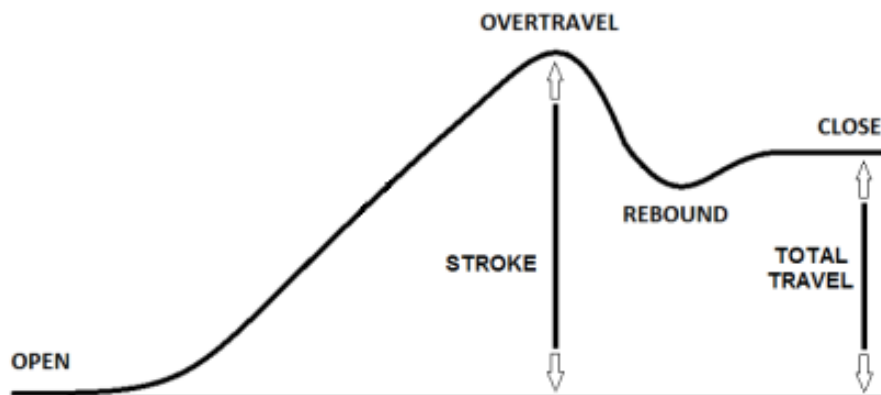


Figure 5.20: Typical closing operation parameters analysed (adapted from [46])

### 5.2.3 Minimum pick-up Voltage

The minimum pick-up measurement is performed to determine the minimum command coil (trip or close) voltage required to operate the circuit breaker. This ensures that the circuit breaker will operate at a specified reduced voltage.

The test procedure determines, at first, a start and stop voltage for the command coil under test. For example, in a 125 VDC command coil, the starting voltage would be 10 VDC and stop voltage 125 VDC. After that, a pulse time should be determined, in order not to overheat the command coil. The dead time, which is the time of pause between pulses, should also be determined, being long enough to assist in the cooling of the command coil. Finally, the voltage step increment is determined, being the amount of voltage that is increased between pulses [46]. Figure 5.21 exemplifies a minimum pick-up voltage test.

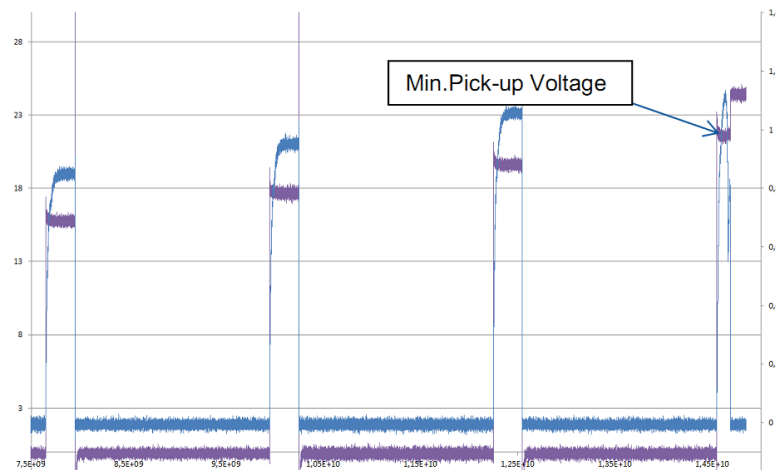


Figure 5.21: Voltage and Current waveforms of a typical minimum pick-up voltage measurement [46]

## 5.3 Summary

In this chapter, the data export from the IED to the numeric computing platform was explained, in order to evaluate the recorded signals.

After the explanation, an online indexing method was suggested through the measurements of the breaker's opening time, current RMS value in the CB after the opening operation and the duration of the TRV. These three parameters were given a weight and summed together to determine an online health index of the breaker in question.

Based on the online health indexing, if the breaker showed signs of weariness or damage, concluded from its total performance score, further offline tests were recommended, based on the state-of-the-art of CB testing in high-voltage substations, which could then conclude if the breaker could still operate or needed maintenance/replacement.

A decision tree of the whole process is shown in Figure 5.22.

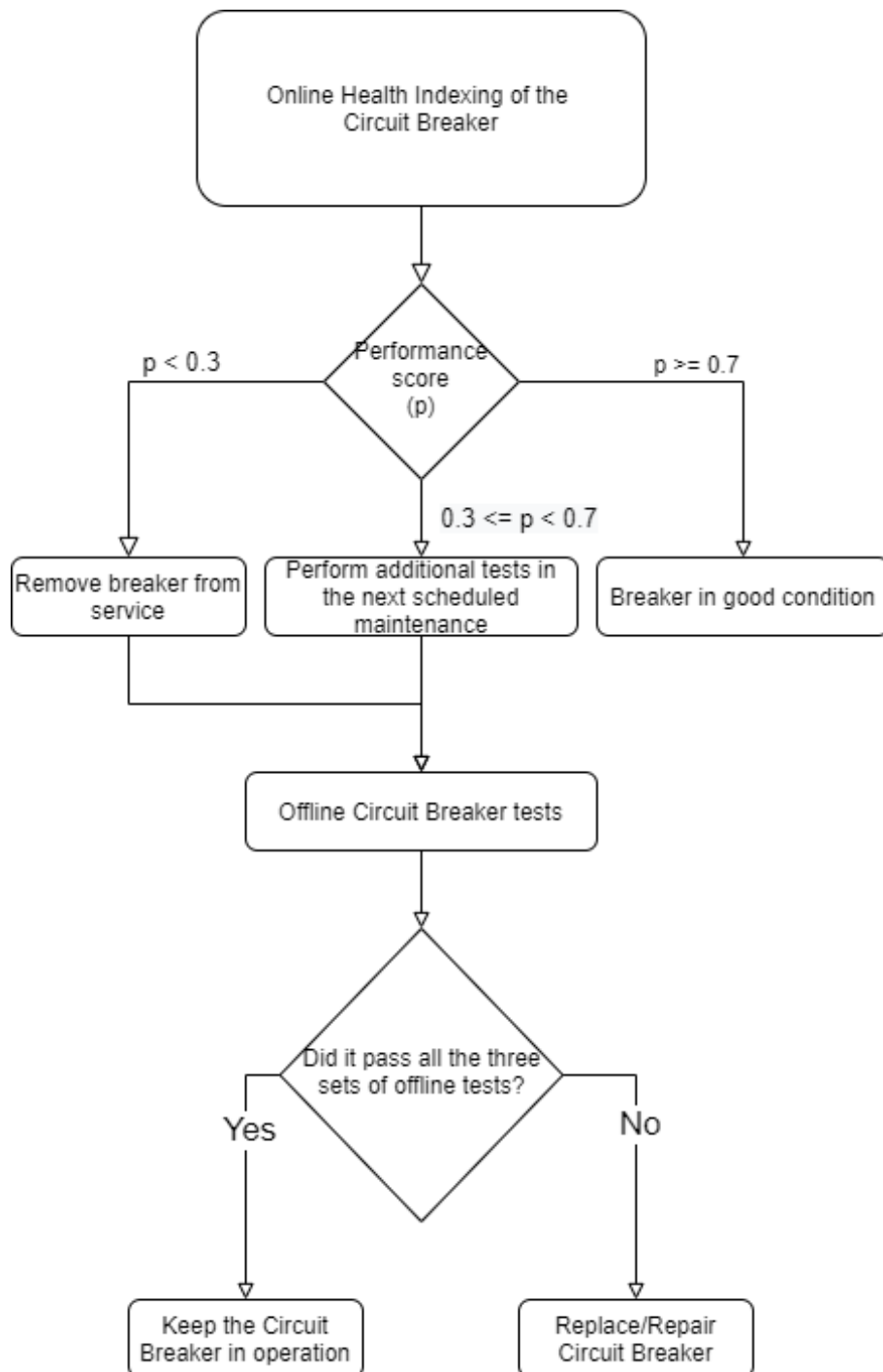


Figure 5.22: Decision tree of the Full Health Indexing of a Circuit Breaker



## Chapter 6

# Main Conclusions and Limitations

Circuit breakers play an important role in the protection of substations and the entire electrical grid. However, in order for them to fulfill their purpose, they need to be in good conditions, being constantly monitored and maintained when something is not functioning properly.

This monitoring is still not done efficiently, as real-time monitoring is still limited in its capabilities in most substations, where the condition of the breaker is not properly verified until it malfunctions, resulting in the shutdown of part of the substation service momentarily due to unexpected maintenance, leading to financial losses.

With the introduction of the IEC 61850 standard, the integration of IEDs in the substations became much easier, allowing all substations to work in a similar manner and improving its communications and overall structure. In addition to that, the COMTRADE standard allowed exporting data from the IEDs in a standardized way, facilitating its acquisition and further analysis.

The process of breaker monitoring data transmitted to the IED, and exporting the data from the IED to a computer for signal processing and analysis can be simulated in a closed-loop scheme, where the behaviour of a CB is modelled, and the resulting voltage and current waveforms can be obtained as the final product.

Using that information, it is possible to create an algorithm defining an online health index of the CB, based on signal parameters such as the opening time of the breaker, the TRV duration or even the current passing through the CB after the opening operation. Subsequently, it is possible to evaluate the overall state of the breaker, concluding if it requires maintenance or additional tests.

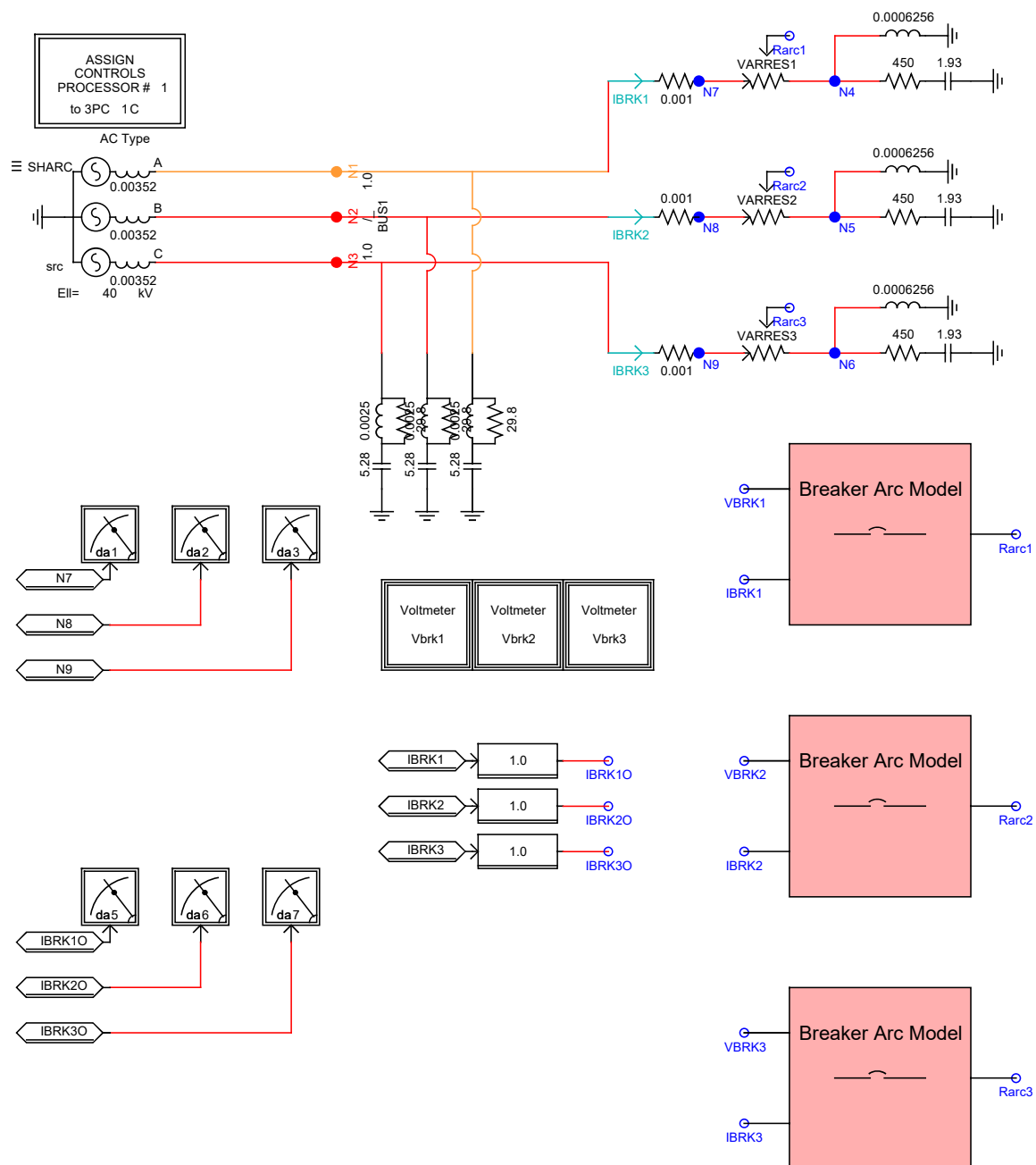
The limitation of this kind of procedure is the information available by just using COMTRADE files. Only the current and voltage signals can be analysed, and parameters such as the SF<sub>6</sub> level or temperatures during operation/standby are not obtainable, not being possible to present a full health status of the CB, and which specific breaker components may be damaged or in risk of malfunctioning.

In addition to that, while simulations are very accurate at representing normal functioning situations, they can differ more from real tests in situations where malfunctioning or other unusual situations are supposed to be simulated, making it more complex to correctly process and analyse the results coming from them.



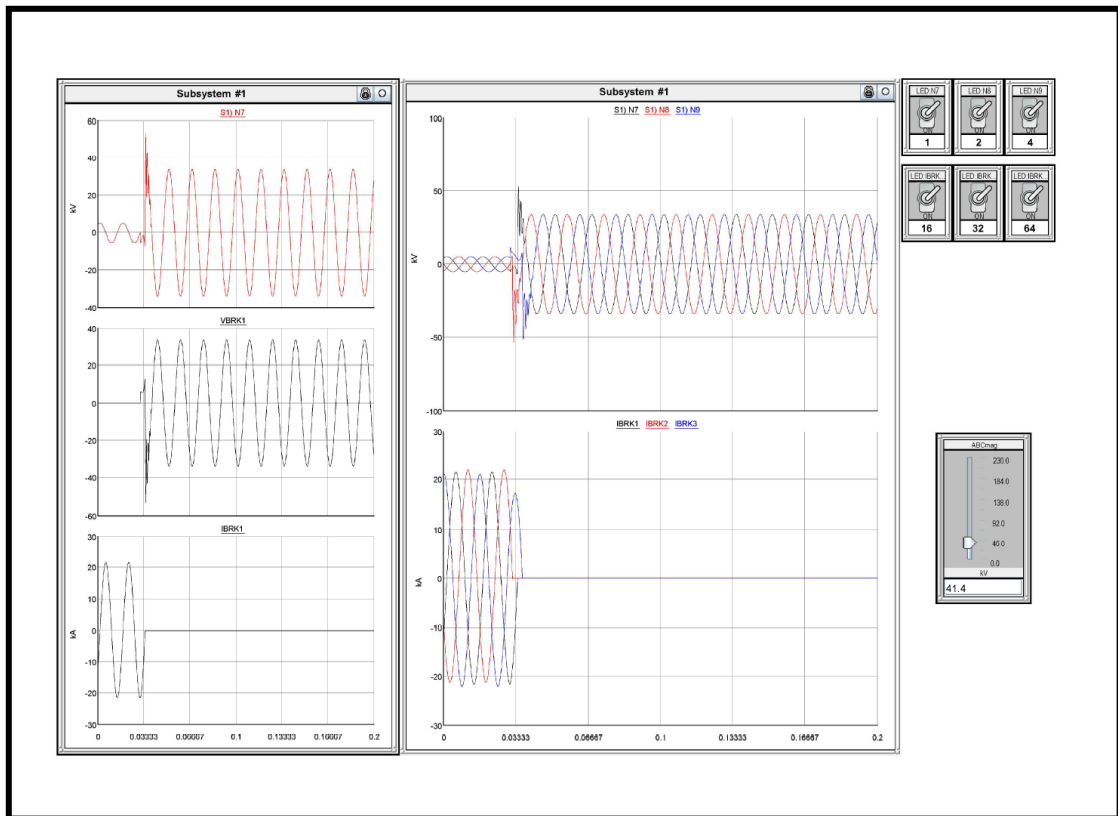
## **Appendix A**

# **RSCAD Draft Scheme**



## Appendix B

# RSCAD Runtime Scheme





# References

- [1] Tushar Kanti Das, Rajesh Debnath, and Sangita Das Biswas. Modeling and implementation of advanced electronic circuit breaker technique for protection. In *Applications of Internet of Things*, pages 15–26. Springer, 2021.
- [2] D. Watkins and G.W. Becker. Substations. In *Standard Handbook for Electrical Engineers*. McGraw-Hill Education, 2018.
- [3] CH Flurscheim. Development of circuit breakers. In *Power circuit breaker theory and design*, page 1. Peter Peregrinus, 1975.
- [4] MP Reece and C Eng. Physics of circuit breaker arcs. In *Power circuit breaker theory and design*. Peter Peregrinus Ltd., 1975.
- [5] E Maggi. S<sub>f</sub>6 circuit breakers. In *IEE Monograph Series*, volume 17, pages 293–317, 1967.
- [6] V. Kamaraju. *Electrical power distribution systems*. McGraw Hill, 8 edition, 2014.
- [7] José Pedro Sucena Paiva. Sobreensões e transitórios electromagnéticos. In *Redes de Energia Eléctrica—Uma Análise Sistémica—2ª Edição*, pages 493–507. Editora IST Press—Lisboa, 2007.
- [8] Ruben D Garzon. *High voltage circuit breakers: design and applications*. CRC Press, 2002.
- [9] Juan A Martinez-Velasco. *Power system transients: parameter determination*. CRC press, 2017.
- [10] D Andersson, M Barrault, D Dufournet, M Hrabosvsky, M Kapetanovic, et al. Applications of black box modeling to circuit breakers. *Electra*, 149:40–71, 1993.
- [11] Otto Mayr. Beiträge zur theorie des statischen und des dynamischen lichtbogens. *Archiv für Elektrotechnik*, 37(12):588–608, 1943.
- [12] AM Cassie. Theorie nouvelle des arcs de rupture et de la rigidité des circuits. *Cigre, Report*, 102:588–608, 1939.
- [13] P.H. Schavemaker and L. van der Slui. An improved mayr-type arc model based on current-zero measurements [circuit breakers]. *IEEE Transactions on Power Delivery*, 15(2):580–584, 2000. doi:10.1109/61.852988.
- [14] E Anke, M Barrault, B Blez, Z Ciok, G Frind, D Dufournet, W Hermann, M Hrabovsky, M Ishikawa, A Kurimoto, et al. Practical applications of arc physics in circuit breakers. survey of calculation methods and application guide. *CIGRE, Electra*, 118:63–79, 1988.

- [15] G. Idarraga Ospina, D. Cubillos, and L. Ibanez. Analysis of arcing fault models. In *2008 IEEE/PES Transmission and Distribution Conference and Exposition: Latin America*, pages 1–5, 2008. doi:10.1109/TDC-LA.2008.4641860.
- [16] Shan Jiang. Pscad component "breaker arc", Sep 2018. [Online; accessed 08-April-2021]. URL: <https://www.pscad.com/knowledge-base/article/262>.
- [17] J.L. Guardado, S.G. Maximov, E. Melgoza, J.L. Naredo, and P. Moreno. An improved arc model before current zero based on the combined mayr and cassie arc models. *IEEE Transactions on Power Delivery*, 20(1):138–142, 2005. doi:10.1109/TPWRD.2004.837814.
- [18] G.A. Cividjian, N.G. Silvis-Cividjian, and J. Klejch. Kema arc model parameters evaluation. In *Proceedings of the 6th International Conference on Optimization of Electrical and Electronic Equipments*, volume 1, pages 215–220, 1998. doi:10.1109/OPTIM.1998.710475.
- [19] U. Habedank. Application of a new arc model for the evaluation of short-circuit breaking tests. *IEEE Transactions on Power Delivery*, 8(4):1921–1925, 1993. doi:10.1109/61.248303.
- [20] King-Jet Tseng, Yaoming Wang, and D.M. Vilathgamuwa. An experimentally verified hybrid cassie-mayr electric arc model for power electronics simulations. *IEEE Transactions on Power Electronics*, 12(3):429–436, 1997. doi:10.1109/63.575670.
- [21] Farshid Salehi, Azade Brahman, Reza Keypour, and Wei jen Lee. Reliability assessment of automated substation and functional integration. In *2016 IEEE Industry Applications Society Annual Meeting*, pages 1–7, 2016. doi:10.1109/IAS.2016.7731952.
- [22] Alex Apostolov, Vice Chairperson, Roy Moxley, G Antonova, J Ariza, Phil Beaumont, Sukuman Brahma, Craig Bryant, J F Burger, J Csisek, Catherine Dalton, T Day, Kevin Donahoe, Fred Friend, J Galanos, Rafael Garcia, Juan Gers, George Gresko, Shinichi Imai, M Janssen, Dylan Jenkins, Jack Jester, Jerry Jodice, M Kezunovic, S Klein, Mike Kockott, L Kojovic, Raluca Lascu, Tony Leszczynski, A Martin, M Meisinger, R Midence, A Mulawarman, Paul Myrda, Pouria Naisani, D Nordell, Damr Novosel, Vajira Pathirana, M Reichard, Imran Rivzi, S Sambasivan, T Sidhu, Mark Simon, T Smith, Dean Sorensen, Farajollah Soudi, Mark Taylor, and Damien Tholomier. Role of Protective Relaying in the Smart Grid Report to the Main Committee. *Working Group C-2 of the System Protection Subcommittee, Power System Relay Committee*, 2017. URL: <http://www.pes-psrc.org/kb/published/reports/PSRCWGC2-RoleofProtectiveRelayingintheSmartGrid.pdf>.
- [23] R. E. Mackiewicz. Overview of iec 61850 and benefits. In *2006 IEEE PES Power Systems Conference and Exposition*, pages 623–630, 2006. doi:10.1109/PSCE.2006.296392.
- [24] J.A. Martínez-Velasco. Computer applications in the electric power industry. In *Standard Handbook for Electrical Engineers*. McGraw-Hill Education, 2018.
- [25] Yiqing Liu, Houlei Gao, Xin Wei, Zhaohong Teng, Peng Wei, Naiyong Li, and Minjiang Xiang. Study on new type of ied with integrated functions in intelligent substation. In *2011 International Conference on Advanced Power System Automation and Protection*, volume 1, pages 161–165, 2011. doi:10.1109/APAP.2011.6180403.



- [26] IEC Standard 61850-6. Communication networks and systems in sub-stations: Part 6: configuration description language for communication in electrical substations related to ieds, 2004.
- [27] Y. Pan. Research on ied configurator based on iec 61850. In *2011 International Conference on Control, Automation and Systems Engineering (CASE)*, pages 1–4, 2011. doi:[10.1109/ICCASE.2011.5997664](https://doi.org/10.1109/ICCASE.2011.5997664).
- [28] Y. Yang, L. Gao, D. N. Zhang, Y. B. Yuan, Q. S. Bu, K. McLaughlin, and S. Sezer. Comparison method for differentiation of iec 61850 based substation configuration files. In *2014 International Conference on Power System Technology*, pages 1796–1801, 2014. doi:[10.1109/POWERCON.2014.6993635](https://doi.org/10.1109/POWERCON.2014.6993635).
- [29] L. Zhu, D. Shi, and P. Wang. Iec 61850-based information model and configuration description of communication network in substation automation. *IEEE Transactions on Power Delivery*, 29(1):97–107, 2014. doi:[10.1109/TPWRD.2013.2269770](https://doi.org/10.1109/TPWRD.2013.2269770).
- [30] B. Bauernschmitt, M. Kaliwoda, B. Keune, D. Hilbrich, and C. Rehtanz. An integral engineering process for centralised protection control systems according to iec 61850-6. In *2015 Modern Electric Power Systems (MEPS)*, pages 1–6, 2015. doi:[10.1109/MEPS.2015.7477158](https://doi.org/10.1109/MEPS.2015.7477158).
- [31] A. Apostolov. Simplifying the configuration of multifunctional distribution protection and control ieds. In *CIREN 2005 - 18th International Conference and Exhibition on Electricity Distribution*, pages 1–4, 2005. doi:[10.1049/cp:20051177](https://doi.org/10.1049/cp:20051177).
- [32] IEC Standard 61850-7-1. Communication networks and systems for power utility automation – part 7-1: Basic communication structure – principles and models, 2020.
- [33] IEC Standard 61850-7-2. Communication networks and systems for power utility automation – part 7-2: Basic communication structure – abstract communication service interface (acsi), 2020.
- [34] Jianqing Zhang and Carl A. Gunter. Iec 61850 - communication networks and systems in substations: An overview of computer science. [Online; accessed 11-June-2021]. URL: <http://seclab.illinois.edu/wp-content/uploads/2011/03/iec61850-intro.pdf>.
- [35] IEC Standard 61850-7-3. Communication networks and systems for power utility automation – part 7-3: Basic communication structure – common data classes, 2020.
- [36] IEC Standard 61850-7-4. Communication networks and systems for power utility automation – part 7-4: Basic communication structure – compatible logical node classes and data object classes, 2020.
- [37] Z. Tang and Y. Zou. Condition monitoring system for circuit breaker based on substation automation system. In *Proceedings of the 41st International Universities Power Engineering Conference*, volume 3, pages 861–865, 2006. doi:[10.1109/UPEC.2006.367603](https://doi.org/10.1109/UPEC.2006.367603).
- [38] Ieee standard common format for transient data exchange (comtrade) for power systems. *IEEE Std C37.111-1999*, pages 1–55, 1999. doi:[10.1109/IEEESTD.1999.90571](https://doi.org/10.1109/IEEESTD.1999.90571).
- [39] RTDS Technologies Inc. *RTDS Hardware Manual*, January 2009.

- [40] RTDS Technologies Inc. *RTDS Power Systems User's Manual*, December 2012.
- [41] G. Bizjak, P. Zunko, and D. Povh. Circuit breaker model for digital simulation based on mayr's and cassie's differential arc equations. *IEEE Transactions on Power Delivery*, 10(3):1310–1315, 1995. doi:[10.1109/61.400910](https://doi.org/10.1109/61.400910).
- [42] Doble Engineering Company. *F6 Multiple Amplifier Configurator Version 5*, October 2015.
- [43] M. Landry, A. Mercier, G. Ouellet, C. Rajotte, J. Caron, M. Roy, and Fouad Brikci. A new measurement method of the dynamic contact resistance of hv circuit breakers. In *2006 IEEE/PES Transmission Distribution Conference and Exposition: Latin America*, pages 1–8, 2006. doi:[10.1109/TDCLA.2006.311501](https://doi.org/10.1109/TDCLA.2006.311501).
- [44] Maryam Khoddam, Javad Sadeh, and Pedjman Pourmohamadiyan. Performance evaluation of circuit breaker electrical contact based on dynamic resistance signature and using health index. *IEEE Transactions on Components, Packaging and Manufacturing Technology*, 6(10):1505–1512, 2016. doi:[10.1109/TCPMT.2016.2601316](https://doi.org/10.1109/TCPMT.2016.2601316).
- [45] Paul Gill. *Electrical power equipment maintenance and testing*. CRC press, 2016.
- [46] Charles Sweetser. A Systematic Approach to High-Voltage Circuit Breaker Testing. Technical report, OMICRON electronics Corp. USA, 2016.